R-05-67

GIS-based modelling of coupled groundwater – surface water hydrology in the Forsmark and Simpevarp areas

Jerker Jarsjö, Yoshihiro Shibuo, Carmen Prieto
Georgia Destouni
Dept. of Physical Geography and Quaternary Geology
Stockholm University

March 2006

Svensk Kärnbränslehantering AB
Swedish Nuclear Fuel
and Waste Management Co
Box 5864
SE-102 40 Stockholm Sweden
Tel 08-459 84 00
+46 8 459 84 00
Fax 08-661 57 19
+46 8 661 57 19

ISSN 1402-3091
SKB Rapport R-05-67

GIS-based modelling of coupled groundwater – surface water hydrology in the Forsmark and Simpevarp areas

Jerker Jarsjö, Yoshihiro Shibuo, Carmen Prieto
Georgia Destouni
Dept. of Physical Geography and Quaternary Geology
Stockholm University

March 2006

Abstract

We here use the PCRaster-POLFLOW approach for quantification of the surface water and shallow groundwater flow systems in the Forsmark and Oskarshamn/Simpevarp areas, updating and extending the results previously reported in R-04-54 (in which, e.g. only the Forsmark area was considered). The modelled flow systems extend all the way to the coast, including 1,532 coastal outlets (with grid-cell resolution 10 m × 10 m) in the modelled Forsmark catchment area of 29.5 km^2 and 6,844 coastal outlets (10 m × 10 m resolution) in the modelled Simpevarp catchment area of 128 km^2.

In both considered areas, each 10 m × 10 m coastal outlet cell has its own sub-catchment. Most sub-catchments are very small, but a relatively small number of coastal outlets have considerably larger sub-catchments and contribute to most of the coastal discharge. For instance, 80% of the total annual average discharge from the considered Forsmark area to the coast flows through only 10 coastal outlets (out of the total 1,532). The corresponding number for Simpevarp is 13 (out of 6,844). The diffuse flow through a large number of modelled coastal outlets also implies that for covering 90% of the total coastal discharge, many more than the major 10 (Forsmark) or 13 (Simpevarp) sub-catchments need to be monitored; for instance, our model results for Simpevarp show that this requires monitoring of approximately 80 mostly relatively small sub-catchments (out of 6,844).

In addition to the above-mentioned coastal discharges, we here deliver predictions of average discharges (annual and seasonal) in hydrological measurement stations within the modelled Forsmark and Simpevarp areas, thus allowing for future direct comparisons with streamflow monitoring, when the measurements have been conducted for long enough to reflect relevant average conditions.

The PCRaster-POLFLOW framework can be used in combination with different evapotranspiration estimation methods or quantifications. We compare two different methods and show that they influence the predictions to a relatively large degree. However, averaging the discharges predicted by the two methods (on the basis of totally uncalibrated site-specific model input parameters), we obtain results that are consistent with available, independent hydrologic runoff data, as previously indicated in R-04-54.

The above-mentioned different results produced by the two tested evapotranspiration methods mainly regard the prediction of mean (or total) outflow, whereas the *relative* distribution of average discharges (annual and seasonal) among the main coastal outlets remains essentially the same for the two tested evapotranspiration methods. Therefore, we can here develop a simple calibration procedure, using one site-specific calibration factor that adjusts for systematic deviations in the predictions of average discharge, without having to calibrate specifically the relative distribution of discharge within the modelled area.

Contents

1 Introduction

This study considers the surface water and shallow groundwater systems in the Forsmark and Simpevarp areas. It constitutes an update and extension of the results previously reported in /Jarsjö et al. 2004/ (hereafter referred to as R-04-54), where the hydrologic process modelling approach PCRaster-POLFLOW /van Deursen 1995, De Wit 1999, 2001/ was used to provide a GIS-based hydrologic model of the Forsmark area.

The PCRaster-POLFLOW approach is used also in the present study. It is based on a single language for performing both GIS and process modelling operations, and allows for analyses of temporally and spatially varying flow and transport processes within the catchment. PCRaster-POLFLOW has previously successfully been applied at relatively large river basins and catchments, such as Rhine, Elbe and Norrström. (See, e.g. /Darracq et al. 2005/ for modelling results on stream water flow and nutrient transport.) Results from the smaller-scale and finer resolution application of PCRaster-POLFLOW at Forsmark reported in R-04-54 showed that the (uncalibrated) PCRaster-POLFLOW model produced results that, on average, agreed well with independent regional estimates of specific runoff.

Here, we present new hydrologic modelling results for the Oskarshamn/Simpevarp area, and update the previously reported (R-04-54) results for Forsmark (that was based on data from July 2003), accounting for recent additions to SKB's database. We also extend the model areas all the way to the coastline, enabling consideration of interactions between surface water – groundwater – seawater systems in future studies. In order to obtain (spatially distributed) evapotranspiration estimates that are consistent with streamflow observations, we also perform site-adaptations of the empirical evapotranspiration relations used in R-04-54, through a new calibration step in the modelling. Comparisons with the previously presented R-04-54 results for Forsmark as well as comparisons between the Forsmark and Simpevarp sites are included in the "conclusion summary" section. Furthermore, the appendix summarises the input file processing and the produced output files, which are available also in electronic format.

2 Objectives

2.1 General objectives

General objectives in the development of site-specific, coupled surface water – groundwater models are to obtain water mass balances that are consistent with observations of precipitation, evapotranspiration and water discharges, on local and catchment scales, and model representations of groundwater recharge and discharge areas that are realistic. Open research questions remain regarding, e.g. the necessary level of detail in the model representation of physical processes that underlie surface water-groundwater exchanges. However, it is clear that trustworthy models of surface water hydrology are necessary for the site-specific understanding of the potential biosphere effects of deep groundwater flows and the effects of surface hydrology on the deep flows.

2.2 Specific objectives

The specific objectives of this study are to

- update the previously reported (in R-04-54) PCRaster-POLFLOW results for the Forsmark area,
- develop a GIS-based PCRaster-POLFLOW surface water model for the Simpevarp area on the basis of available geographic, hydrological and hydrogeological data in SKB's database, and,
- perform site-adaptations (considering Forsmark and Oskarshamn independently) of the used empirical evapotranspiration relations, resulting in site-specific maps with local (cell by cell) evapotranspiration and precipitation surplus values that reproduce stream-flow observations when used as input for the subsequent hydrological modelling step.

We then **hypothesise** that the PCRaster-POLFLOW surface water modelling approach can be applied to the Oskarshamn area, and reproduce the surface water hydrological observations there. We furthermore hypothesise that the predictions of the *relative* distribution of coastal flows from the Oskarshamn catchment(s) can be shown to be independent of the two evapotranspiation models used in /Jarsjö et al. 2004/, in accordance with previous results from the Forsmark area.

3 The numerical modelling approach

3.1 Overview of the modelling procedure

In addition to the methods and procedures previously described in R-04-54, we here use a calibration step in the calculations. This calibration implies that the actual evapotranspiration E_a is estimated and used as input to a first, uncalibrated model run. Based on the ratio between the runoff predicted by this uncalibrated model, and the measured (or independently estimated) runoff, the E_a-input is altered (being considered as more uncertain than, e.g. precipitation) according to Equation (4) below. This altered E_a input is then used in a second model run, producing a calibrated runoff that is consistent with the measurements. In this application, uncalibrated model results were obtained by E_a-method (ii), however, we expect that similar calibration procedures to the one detailed below can be applied also for other estimation methods.

3.2 Calibration of actual evapotranspiration E_a using total runoff q

In Sections 5.1 and 7.1, we show that the (uncalibrated) PCRaster-POLFLOW model produces results that, on average, agree well with independent "regional" estimates based on measurement data in the surroundings of Forsmark and Simpevarp. However, even though the results on average were consistent with measurements, the differences between the two approaches (E_a-method (i) and E_a-method (ii), see further R-04-54) were considerable. The empirical E_a-method (ii) /Wendland 1992/ was based on conditions in German catchments and overestimates the evapotranspiration in our Swedish applications, presumably because of the colder climate in Sweden. In this section, we therefore outline a methodology to perform site-adaptations (considering Forsmark and Simpevarp independently) of the used empirical evapotranspiration relations. The results of the site-adaptations are presented in Sections 5.5 and 7.5.

Our starting point is to consider E_a-method (ii), which relates E_a to different soil and vegetation conditions (see Table 3-1) and therefore yields more realistic spatial variations in E_a than the alternative temperature method (i) /Langbein 1949, Turc 1954, Meinardi et al. 1994/. Our working hypothesis, which is based on the result that the relative coastal outflows among the different catchment outlets in Forsmark and Simpevarp remained the same for both the tested E_a-estimation methods (see Sections 5.2 and 7.2 of this report and the results in R-04-54) is that all the E_a-coefficients of /Wendland 1992/ can generally be adjusted through multiplication of the same, single, site-specific (calibration) factor, such that the observed flows within the catchment then are reproduced.

Since the hydrologic data monitoring programmes in Simpevarp and Forsmark started rather recently, detailed site-specific data representative for long-term average conditions are presently lacking. Once the initialised field measurements have been running for several years, their data can preferably be used in the calibration procedure. However, as for now, we use the experience from previous Swedish PCRaster-POLFLOW applications, that a good estimation q_{est} of independently measured runoff can be obtained by considering the average runoff produced by E_a methods (i) and (ii) i.e. $q_{est} = (q_{(i)}+q_{(ii)})/2$ (this was the case for, e.g. for the Norrström catchment; /Greffe 2003, Darracq 2003, Darracq and Destouni 2005, Darracq et al. 2005/ and for the Forsmark and Simpevarp catchments, as shown in this report and in R-04-54). This average runoff will be used as target for the calibration.

Table 3-1 shows the original, empirically obtained E_a-values for different soil and vegetation conditions in German catchments. In R-04-54, the peat class is lacking, as it is in /Meinardi et al. 1994/. Here, we include the peat class, in analogy with the results reported by /Wendland 1992/. As in R-04-54, in cases when the estimated E_a was greater than 90% of the local P-value (using either method (i) or (ii)), the relation $E_a = 0.9 \times P$ was used instead of the method (i) or (ii) estimation. In practice, for the considered catchments, the $E_a = 0.9 \times P$ relation was used relatively seldom. For instance, for the Forsmark area, the relation was not used at all in the method (i) application, and for 13% of the pixels in the method (ii) application, then applying mainly to areas classified as water.

Table 3-1. E_a-values as a function of soil texture and land cover (method (ii); /Wendland 1992/).

Soil texture:	E_a(mm/year)	
Land cover:	Forest	Other land cover
Very fine	570	550
Fine	550	470
Medium fine	530	423
Medium	475	375
Coarse	450	325
Peat	n.a.	520
Water	n.a.	600

n.a. = not applicable.

The average precipitation surplus PS (mm/year) over an entire catchment, using the original E_a method (ii) with the coefficients according to Table 3-1 is given by:

$$\overline{PS}^{(ii)} = \frac{1}{n_{pixel}} \left(\sum_{npixel} P - \sum_{npixel} E_a^{(ii)} \right) \quad (1)$$

where n_{pixel} is the total number of grid cells (or pixels) representing the catchment, P is the annual precipitation (mm/year) over the considered grid cell, E_a (mm/year) is the annual actual evapotranspiration from the grid cell according to Table 3-1 and superscript (ii) refers to the use of E_a-method (ii).

Multiplying now all the empirical coefficients of Table 3-1 by a single calibration factor X^{cal}_{Ea}, a corresponding calibrated average PS is given by:

$$\overline{PS}^{cal} = \frac{1}{n_{pixel}} \left(\sum_{npixel} P - X^{cal}_{Ea} \sum_{npixel} E_a^{(ii)} \right) \quad (2)$$

We note that $\overline{PS}$ is equal to the specific runoff q that can be derived from the model output (through dividing the total runoff Q by the catchment area A), since both groundwater and surface water flows are included in q. We further let r_q quantify the ratio between the actual runoff and the uncalibrated runoff. It then follows that the ratio between the calibrated $\overline{PS}$

in Equation (2) and the method (ii) $\overline{PS}$ given by Equation (1) must be equal to r_q in order to reproduce the assumed correct runoff through the calibration, yielding:

$$\frac{\sum_{npixel} P - X_{Ea}^{cal} \sum_{npixel} E_a^{(ii)}}{\sum_{npixel} P - \sum_{npixel} E_a^{(ii)}} = r_q \qquad (3)$$

In our case, in absence of site-specific long term measurements, we estimate the actual runoff as $q_{est} = (q_{(i)}+q_{(ii)})/2$ (see also above discussion), where $q_{(i)}$ is the specific runoff produced by method (i) and $q_{(ii)}$ is the specific runoff produced by method (ii). The ratio r_q between the assumed correct runoff (or target runoff) and the method (ii) runoff is then $r_q = q_{est}/q_{(ii)}$. The single calibration factor X^{cal}_{Ea} (by which all the E_a-coefficients of Table 3-1 should be multiplied with in order to represent site-specific conditions) can now be determined as:

$$X_{Ea}^{cal} = r_q + (1 - r_q) \frac{\sum_{npixel} P}{\sum_{npixel} E_a^{(ii)}} \qquad (4)$$

In summary, the X^{cal}_{Ea} term in Equation (4) expresses how much the uncertain total evapotranspiration used as input to an uncalibrated model run (here based on evapotranspiration from E_a-method (ii); Table 3-1), must be modified in order to obtain, in a second model run, a calibrated runoff that is consistent with measurements (or independent estimations). The basis for this correction is r_q, which in practice can be obtained as the ratio between the measured (or independently estimated) site specific runoff and the runoff from the uncalibrated model run (here taken as $r_q = q_{est}/q_{(ii)}$).

For example, considering the here used E_a-method (ii), which was developed for German conditions, the calibrated evapotranspiration is expected to be smaller in Sweden than implied by the uncalibrated method (ii) evapotranspiration given in Table 3-1 (i.e. $X^{cal}_{Ea} < 1$) because of the colder climate in Sweden (as previously mentioned). Therefore, the actual runoff is expected to be larger than the uncalibrated method (ii) runoff, yielding some (site-specific) $r_q > 1$. Given these conditions, Equation (4) accounts for the fact that the correction/calibration coefficient X^{cal}_{Ea}, which importantly relates to the evapotranspiration term only, must be lowered more below unity the smaller and hence less dominating evapotranspiration is in relation to precipitation (i.e. the more $\Sigma P/\Sigma E_a^{(ii)}$ is above unity), in order to alter (calibrate) the model runoff by the (fixed and site-specific) ratio r_q. This approach is hence primarily meaningful from a physical viewpoint if the uncertainties in E_a are much greater than the uncertainties in P; otherwise, similar manipulations to the P-input might as well be considered.

4 Update of Forsmark application: The catchment and input data

4.1 Model area, digital elevation model and streams

The updated results are based on the version 1.2 digital elevation models for the site investigation programme in Forsmark /Brydsten and Strömgren 2004/. The original digital elevation was changed according to the summary in the appendix and the previous description in R-04-54 (however, in contrast to R-04-54, the catchment boundary is here given through the digital elevation model).

The model area was extended all the way to the coastline (which was not the case in R-04-54), enabling consideration of interactions with seawater in future studies. As a result, a large number of very small coastal sub-catchments are now included in the model area and the number of coastal outlets increased from 11 (in the previous study) to 1,532 (here). Figure 4-1 shows the catchment boundary, streams, and location and ID of the 10 out of the 1,532 outlets with the highest flow values. These 10 outlets contribute to approximately 80% of the total annual average discharge Q_{TOT}, with local stream discharge $Q_i > 0.01Q_{TOT}$ at each location. For comparison, we used the same criteria for identifying the most important outlets in Simpevarp, resulting there in a total of 13 outlets (Section 6.1). The total modelled catchment area is 29.46 km^2. The locations of the measurement stations are shown in Figure 5-9.

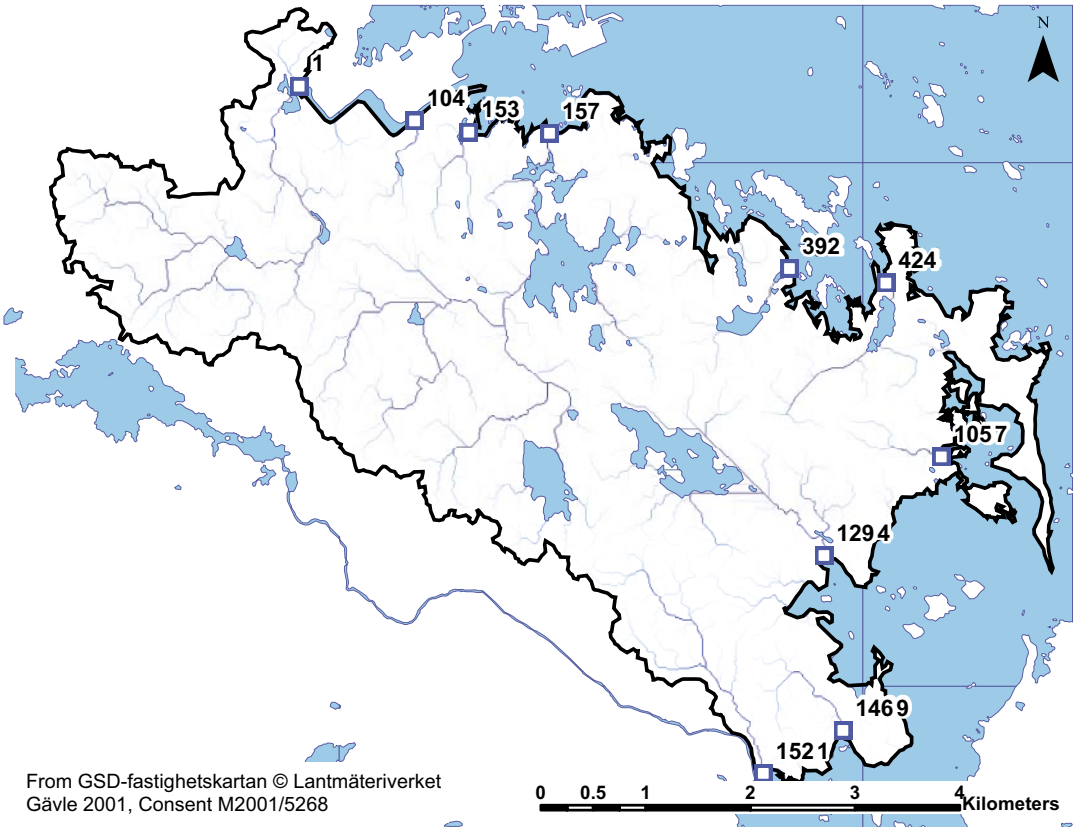

Figure 4-1. *Location of catchment boundary (black line) and streams (blue lines), as well as location and ID of the top ten coastal outlets with regard to high discharge values, out of the 1,532 outlets.*

4.2 Precipitation, temperature and evapotranspiration

The here used precipitation and temperature inputs are identical to those described in R-04-54 (summarised in /Larsson-McCann et al. 2002a/). Furthermore, the estimation of actual evapotranspiration according to the two independent methods (i) and (ii) follows the description in R-04-54.

4.3 Soil data

The SKB v 1.2 dataset contains new soil data for the central part of the model area, and the R-04-54 results are here updated accordingly. However, the new dataset does not include the westernmost and southernmost parts of the model area. Therefore, in these regions, the same soil data set is used as in R-04-54. The coverage of the new dataset is illustrated in Figure 4-2.

The translation of the soil classes into the soil texture classes needed as input for the PCRaster-POLFLOW model is shown in Table 4-1, which includes more soil classes than the corresponding table in R-04-54, due to the larger number of classes in the v 1.2 soil dataset. The resulting soil texture map, used as input for the updated model, is shown in Figure 4-2.

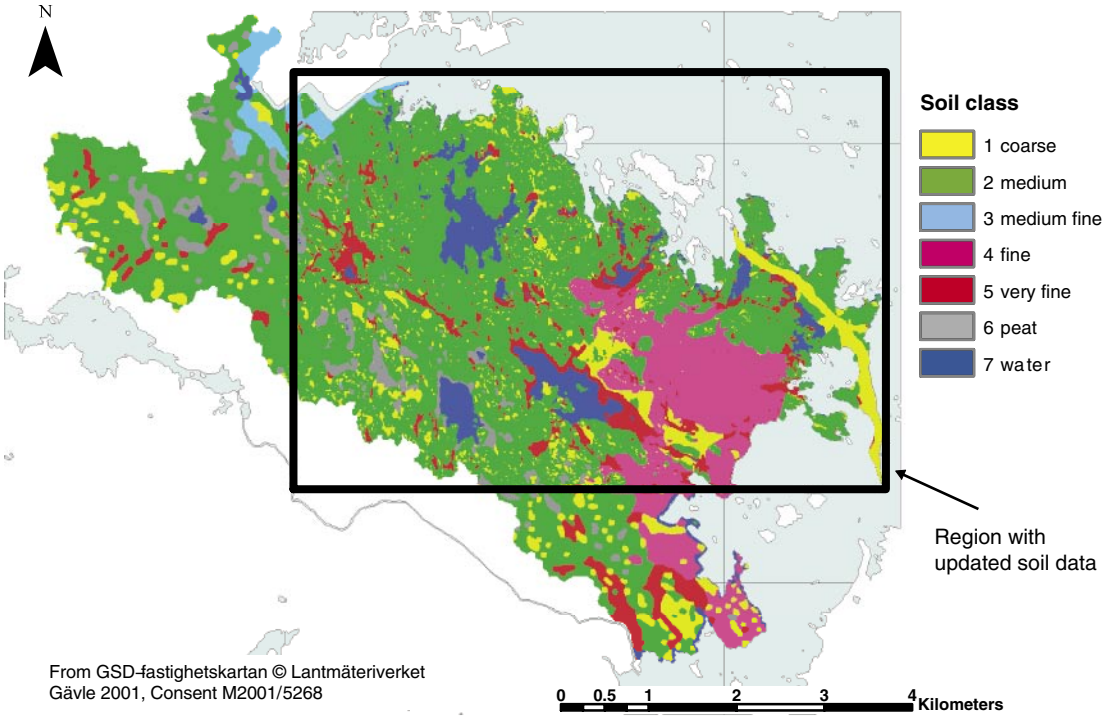

Figure 4-2. *The soil texture map for Forsmark, used as input for the hydrological modelling. Derived on basis of the SGU soil type map "Jordartsinformation i serie Ae" translated as in Table 4-1. The black rectangle shows the coverage of the updated soil dataset.*

Table 4-1. Translation of the soil categories in the SGU coding "J123" to the six soil texture classes required by the empirical relations used in this work, considering the Forsmark area.

Soil category given in the SGU classification "J123"	J123 code	Soil texture (translated)	PCRaster index
Glaciofluvial sediment, coarse silt – boulder	50	coarse	1
Till on glaciofluvial sediment, course silt – boulder	59	coarse	1
Rock	92	coarse	1
Surge sediment, gravel	33	coarse	1
Surge sediment, gravel with thin surface layer of peat	433	coarse	1
Surge sediment, sand	30	coarse	1
Surge sediment, sand with thin surface postglacial sediment, clayey gyttja – gyttja clay	9403	coarse	1
Surge sediment, sand with thin surface peat layer	430	coarse	1
Surge sediment, stone – boulder	34	coarse	1
Bedrock	890	coarse	1
Bedrock with thin surface till layer, sandy	4111	coarse	1
Bedrock with thin surface surge sediment, sand	4113	coarse	1
Bedrock with thin surface peat layer	4112	coarse	1
Sandy till	95	medium	2
Sandy till with thin surface layer of glacial clay, unspecified	9491	medium	2
Sandy till with thin postglacial sediment, clayey gyttja – gyttja clay	9490	medium	2
Sandy till with thin surge sediment, sand	9489	medium	2
Sandy till with thin surface peat layer	495	medium	2
Fillings on unknown subsurface	290	medium fine	3
Clayey sandy silty till	96	fine	4
Clayey sandy silty till with thin surge sediment, sand	9487	fine	4
Clayey sandy silty till with thin surface peat layer	496	fine	4
Glacial clay, unspecified	40	very fine	5
Glacial clay, unspecified with thin surface postglacial sediment, clayey gyttja – gyttja clay	9405	very fine	5
Glacial clay, unspecified with thin surface surge sediment, gravel	9402	very fine	5
Glacial clay, unspecified with thin surface surge sediment, sand	9401	very fine	5
Glacial clay, unspecified with thin surface peat layer	440	very fine	5
Mud	6	very fine	5
Clayey gyttja – gyttja clay	16	very fine	5
Clayey gyttja – gyttja clay with thin surface peat layer	416	very fine	5
Post-glacial clay, unspecified	17	very fine	5
Post-glacial clay, unspecified with thin surface postglacial sediment, clayey gyttja – gyttja clay	9406	very fine	5
Fen peat	5	peat	6
Bog peat	1	peat	6
Water	91	water	7

4.4 Land cover (vegetation) data

Updated groundlayer and vegetation data was provided to us in processed form by SKB as ArcGIS shape files (from the vegetation mapping of /Boresjö Bronge and Wester 2003/; see also Appendix 1). The altogether 12 considered original groundlayer and vegetation classes were reduced to the five land cover classes required by PCRaster-POLFLOW according to Table 4-2.

Table 4-2. Translation of 12 original vegetation and groundlayer classes to 5 new land cover classes required by the empirical relations used in this work, considering the Forsmark area.

Original class	Class code	Land cover (translated)	PCRaster index
Built-up	14,15,16	Built-up/rock	1
Bare rocks	*	Built-up/rock	1
Deciduous forest	19	Forest	3
Forest, conifers and mixed	2	Forest	3
Other open land	5,17	Open land	2
Clear-cut	6	Open land	2
Arable land	4	Open land	2
Wetland	*	Wetland	4
Water	1	Water	5

* Additional class from separate shape file, see further Appendix 1.

The resulting land cover map, used as input for the updated model, is shown in Figure 4-3. In comparison with previous input, the area of the water class (number 5) decreased, whereas the open land class (number 2) increased.

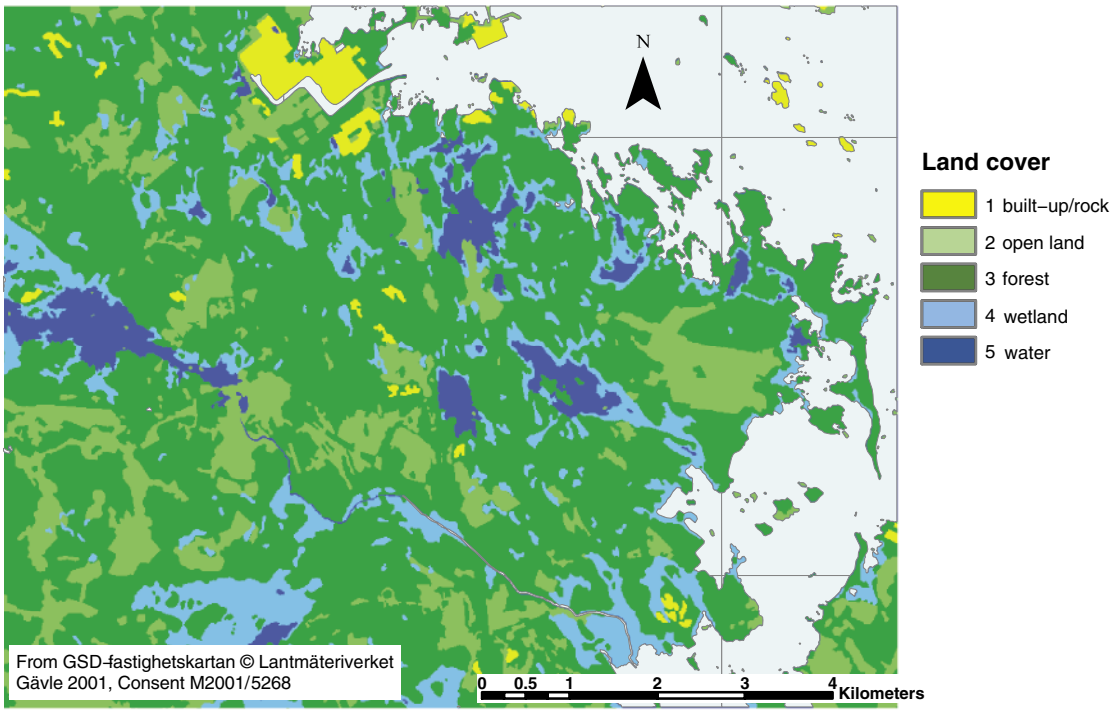

Figure 4-3. The land cover map for Forsmark, used as input for the hydrological modelling.

5 Update of Forsmark application: Results

5.1 Precipitation surplus and runoff

Figure 5-1 shows the updated evapotranspiration (in mm/year) using (a) estimation method (i), and (b) method (ii). The result is consistent with the one previously reported in R-04-54, although these updated values are slightly lower for method (ii) (Figure 5-1b) than in R-04-54. (Note the different scales in (a) and (b)).

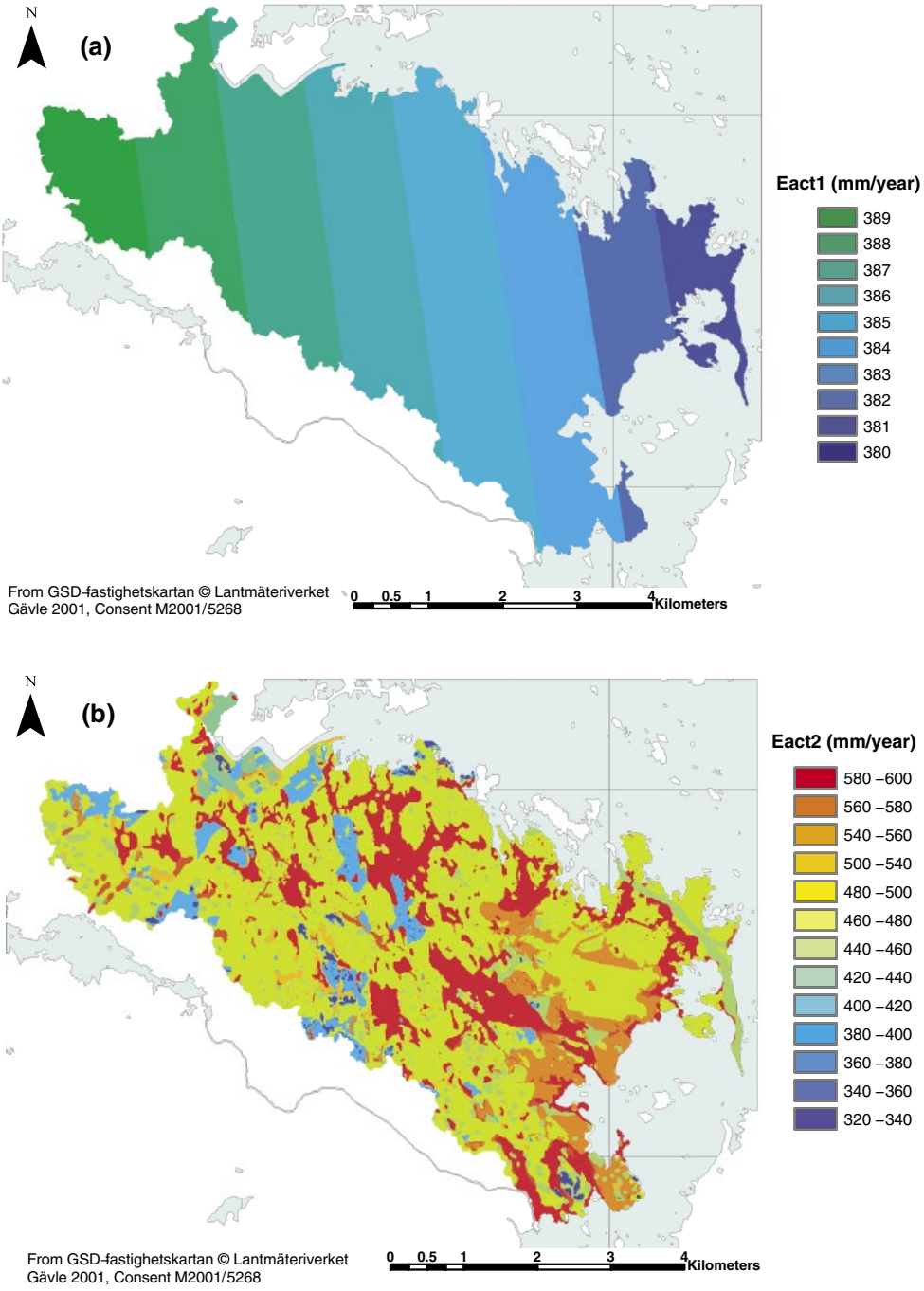

Figure 5-1. *Calculated evapotranspiration (in mm/year) using (a) method (i), and (b) method (ii).*

The precipitation surplus maps of Figure 5-2 are also similar to the previously reported ones, although these updated values are slightly higher for method (ii) (Figure 5-2b) than in R-04-54.

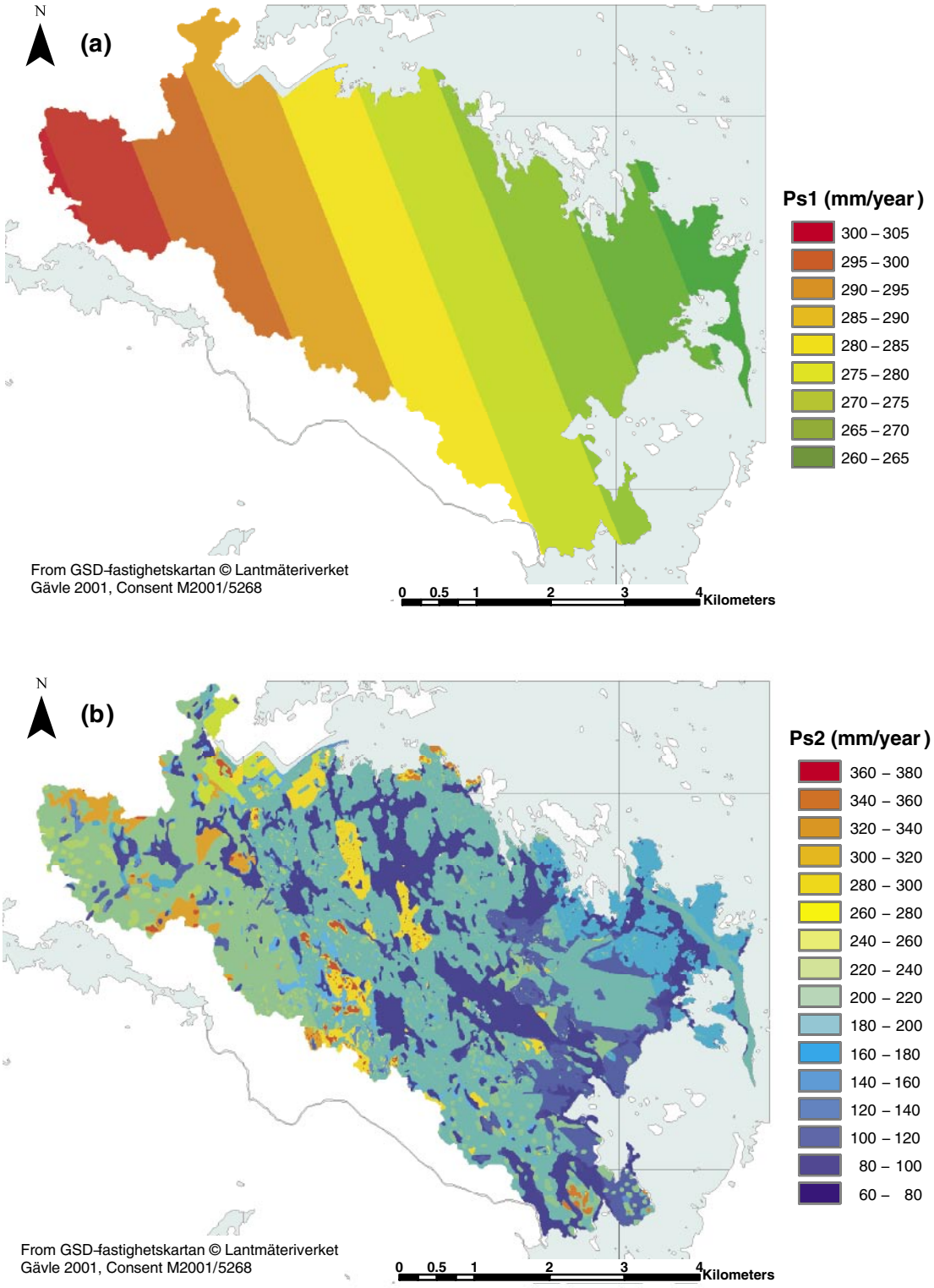

Figure 5-2. *Calculated local precipitation surplus (in mm/year), PS, which also equals total locally created runoff, R (Equation (2)), using (a) evapotranspiration method (i), and (b) evapotranspiration method (ii).*

Figure 5-3 shows the estimated local groundwater recharge index, and Figures 5-4 (a) and (b) show the resulting local groundwater recharges using E_a-estimation methods (i) and (ii), respectively. The patterns and values presented in these figures are consistent with the previous results, with the only readily noticeable difference being that the extent of the areas characterized by the very lowest values (dark blue in the figures) decreased, because the area of the water class in the input decreased (see Section 4.4).

Averaging the local PS values shown in Figure 5-2 for the entire catchment area, we obtained updated values for the specific runoff of the catchment, shown in Table 5-1. The values are on average slightly higher (by 7%) than the previously reported ones (in R-04-54), with in particular the method (ii) value being 17% higher than the one in R-04-54. This can be due to differences in the model extent (which influences both the method (i) and method (ii)-estimates) and differences in soil texture and land cover input (which only affects the method (ii) estimate). We can hence conclude that most of the differences must be due to the use of more detailed information on the soil and land characteristics in the present update. Independently estimated area-averaged runoff values for the Forsmark catchment were on average 7.1 l/s/km^2 (see Table 5-2 of R-04-54), which is close to the here reported average value of 7.2 l/s/km^2.

Table 5-1. Update of modelled area-averaged (i.e. specific) runoff in the Forsmark catchment using different evapotranspiration estimation methods (i) and (ii).

Specific runoff	Prediction method	Main input variable(s)
8.94 l/s/km^2	Method (i)	Temperature
5.40 l/s/km^2 l/s/km^2	Method (ii)	Soil type and land cover
Average: 7.17 l/s/km^2	–	–

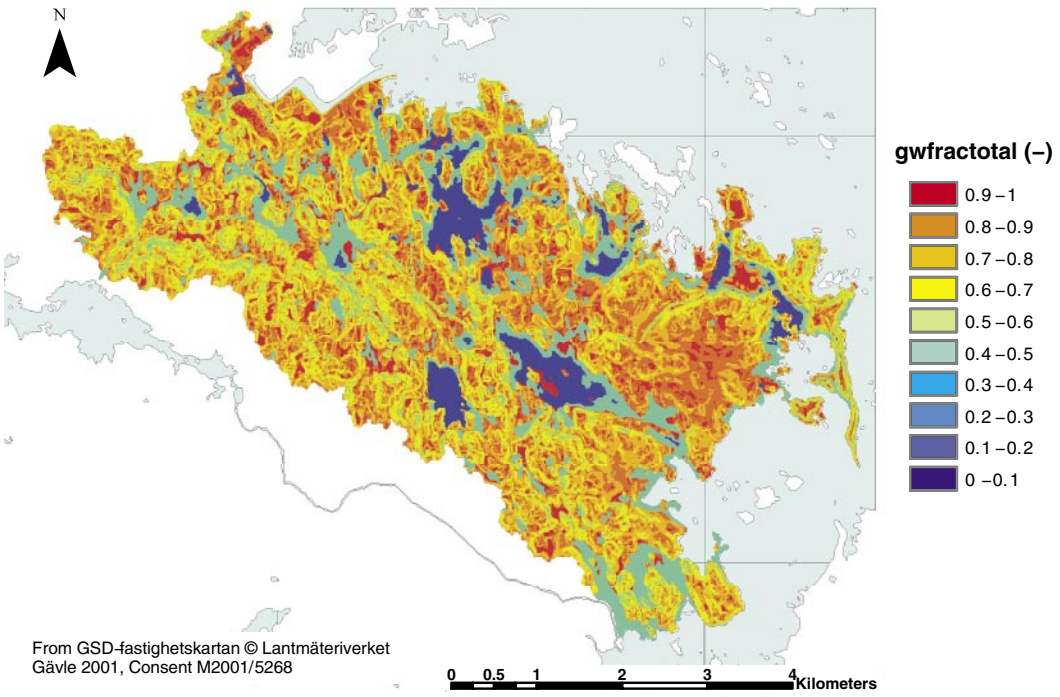

Figure 5-3. *The calculated groundwater recharge index, f_{gw} (dimensionless fraction of precipitation surplus, PS (Figure 5-2); Equation (9) in R-04-54).*

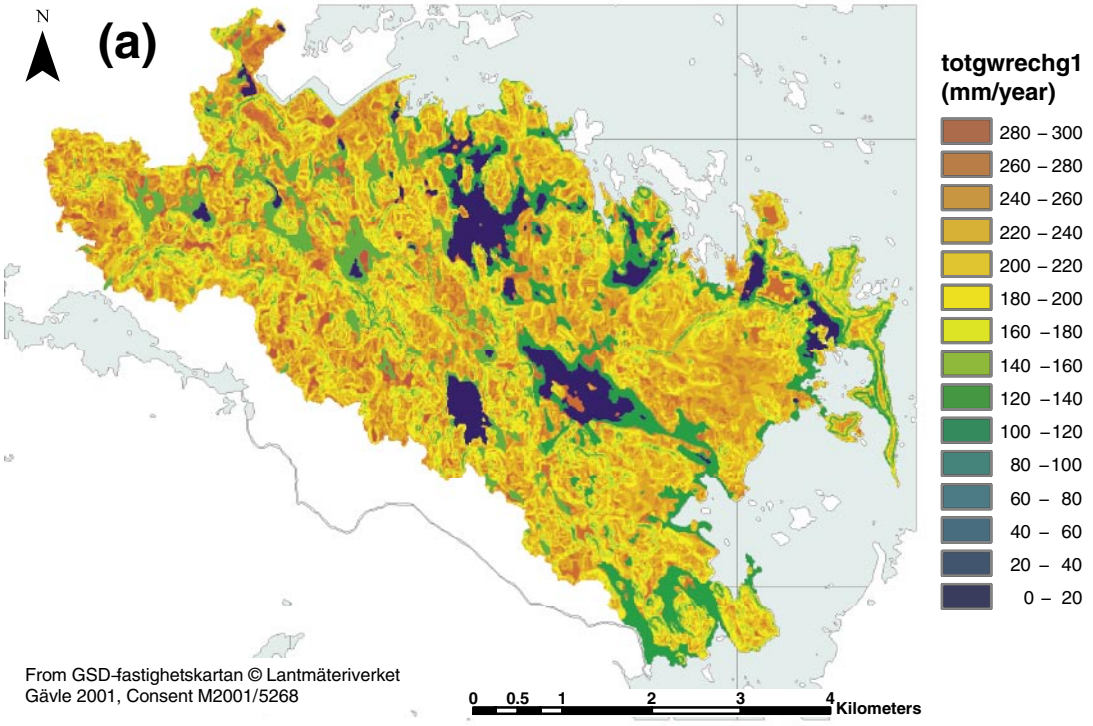

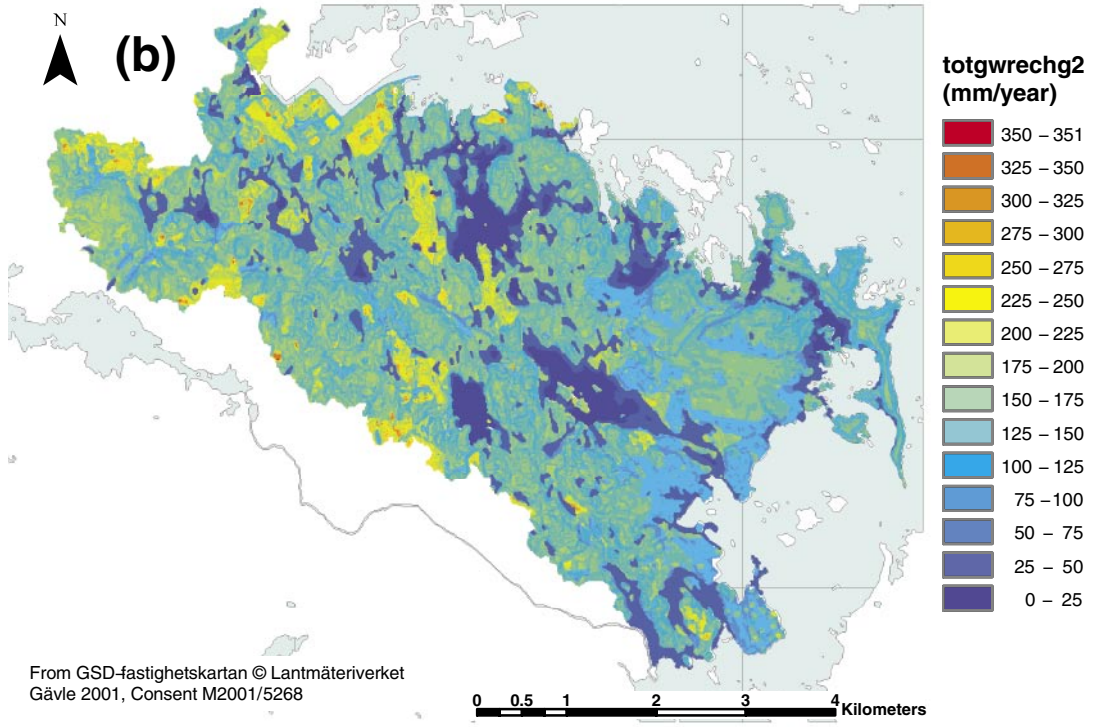

Figure 5-4. *Calculated local groundwater recharge, GW (in mm/year), and corresponding locally created groundwater discharge R_{GW} = GW, using Equation (3) in R-04-54 and* ***(a)*** *E_a-method (i), or* ***(b)*** *E_a-method (ii).*

5.2 Streamflow distribution among different coastal outlets

Since the model area was extended all the way to the coastline (which was not the case in R-04-54), the number of coastal outlets increased from 11 (in R-04-54) to 1,532 (here), with each of the numerous new outlets mainly representing (very) small, coastal sub-catchments without permanent streams.

Figure 5-5 shows the calculated streamflow, Q (Equation (6) in R-04-54) for the top 10 outlets with regard to high Q-values (see Figure 4-1 for their location), out of the 1,532 outlets. These 10 outlets together contribute to 80% of the total coastal discharge from the modelled area. The discharge values of the two dominating outlets (1 and 157) are slightly higher than in R-04-54. One of the causes for this, in addition to the previously mentioned effect of the higher area-averaged runoff, is probably that the outlets now are situated at the coast, rather than at inland locations. Therefore, the coastal land strip now also contributes to the flow.

In R-04-54, it was shown that E_a-methods (i) and (ii) yield the same *relative* flows, i.e. the same relative distribution of total flow among the there considered 11 different coastal outlets (and associated sub-catchments) of the total catchment area. Here, we have 1,532 different outlets, and therefore, we consider in Figure 5-6 only the ten outlets that contribute the most to the total flow. Figure 5-6 shows that the pattern for these ten outlets is consistent with the results previously reported in R-04-54.

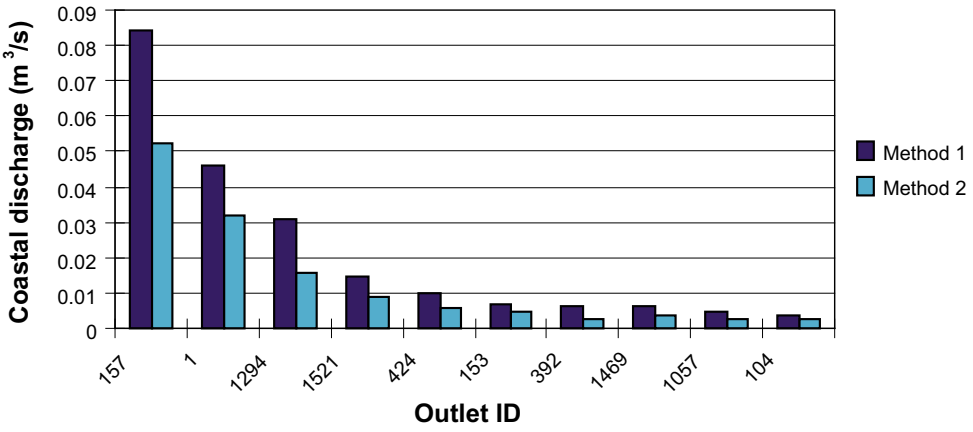

Figure 5-5. *Estimated coastal stream discharge Q (Equation (6) in R-04-54) through the 10 largest coastal stream outlets within the Forsmark area (contributing to 80% of the total discharge from the area; see Figure 4-1 for their location) for Ea-method (i) (dark blue bars) and Ea-method (ii) (light blue bars).*

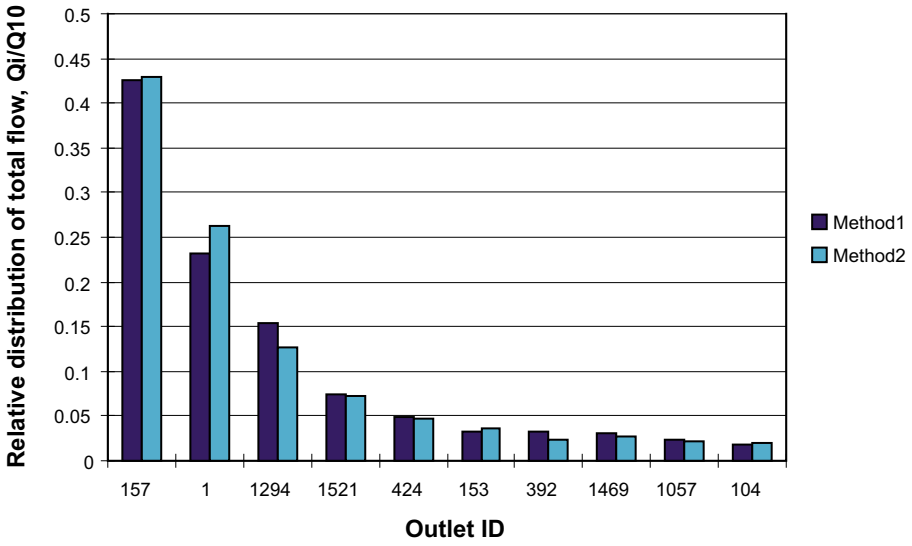

Figure 5-6. *Relative distribution Q_i/Q_{10} of the sum of flow for the ten selected Forsmark outlets Q_{10} among these outlets i (i = 1 to 10), for E_a-method (i) (dark blue bars) and E_a-method (ii) (light blue bars).*

5.3 Average seasonal stream flow in coastal outlets

The estimated average seasonal coastal discharge for the Forsmark area is shown in Figure 5-7, with the considered winter-season being an 8-month period between 1st of October and 31st of May, and the summer season being a 4-month period between 1st of June and 30th of September. Through this definition, the change in snow storage between the beginning and end of each season is expected to be zero on average (therefore not modelled). The modelling accounts for average differences in precipitation and evapotranspiration between the considered seasons (temperature effects implicitly accounted for; see R-05-54 for details). For simplicity, it is assumed that the total changes in surface water and groundwater storage within each season is small. The updated results are similar to the results in R-05-54, with the calculated average coastal discharge within the summer season (blue bars in Figure 5-7) being slightly less than half that of the winter season (grey bars).

Since method (i) appears to generally overpredict the average annual precipitation surplus and runoff (with a predicted value of 8.9 l/s/km^2 in comparison with the independently estimated average value of 7.1 l/s/km^2; see R-04-54), it is likely that also these uncalibrated estimates of seasonal discharges are biased to a similar extent. However, since the coastal results show the same relative distribution of total flow Q10 among the selected 10 outlets during both the winter season and the summer season (Figure 5-8), one single calibration factor would be sufficient to correct for such systematic bias in all 10 selected coastal outlets (characterised by the largest discharges among all outlets). This hence implies that the calibration methodology outlined in Section 3.1 may be relevant also for estimation of seasonal conditions, at least in the larger catchments.

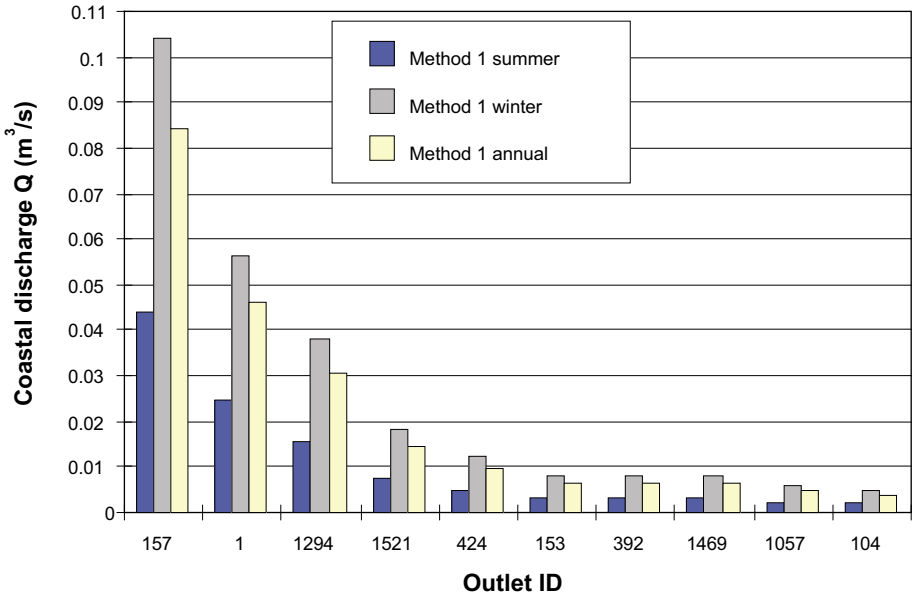

Figure 5-7. *Average, seasonal coastal discharge in summer (blue bars) and winter (grey bars), using method (i) (for the 10 outlets with largest discharge). For comparison, the light yellow bars show the annual average discharge values predicted by method (i).*

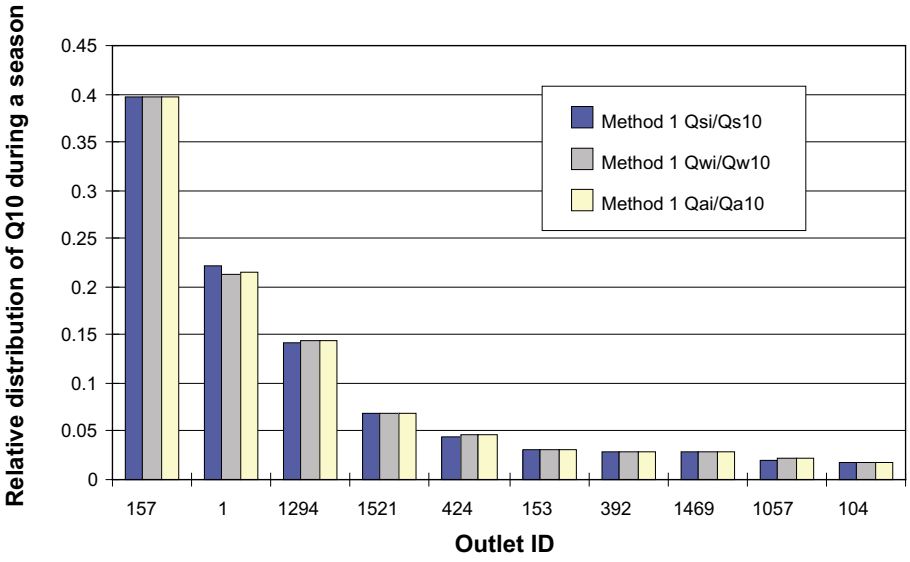

Figure 5-8. *Relative distribution of total average seasonal discharge Q10 among the 10 largest coastal outlets. The blue bars show results for the summer season (indicated by index s) for each outlet i (Qsi/Qs10, where Qsi is the flow at each coastal outlet and Qs10 is the sum of flow from the 10 considered outlets), the grey bars show results for the winter season (indicated by index w; Qwi/Qw10), and the light yellow bars show results for the average annual discharge (index a; Qai/Qa10).*

5.4 Stream flow in measurement stations

The locations and IDs (VP1–VP4) of planned measurement stations considered in report R-04-54 is in Figure 5-9 compared with updated locations and IDs (201–204) of the installed measurement stations, used here. Station 201 was previously denoted VP4, station 202 was denoted VP1, station 203 is situated upstream of the previous VP2 and station 204 is situated upstream of previous VP3.

Figure 5-10 shows our updated, expected best estimate of the average annual discharge Q (Equation (6) in R-04-54). This estimate is based on the averaging of the flow results from methods (i) and (ii), with basic results of estimation methods (i) and (ii) being listed in Table 5-1. As discussed in previous sections and in /Greffe 2003/, the mean value of (uncalibrated) method (i) and (ii) predictions have been shown to agree well with experimental observations in, e.g. the Norrström catchment. For the two stations 202 (VP1) and 201 (VP4) that have the same location as in R-04-54, the updated results of Figure 5-10 show approximately 10% higher flows (at these specific points) than in R-04-54, which must attributed to the updated input data (digital elevation model, soil and land cover data, see Chapter 4).

The above-used averaging procedure reduces systematic errors that seem to be associated with each of the two methods when applied to Swedish catchments. This implies that there is a need for model calibration. We therefore apply a (re-) calibration procedure, considering method (ii) (originally calibrated for German conditions). In the present lack of site-specific hydrologic monitoring results for long-term average conditions, on which calibrations pref-

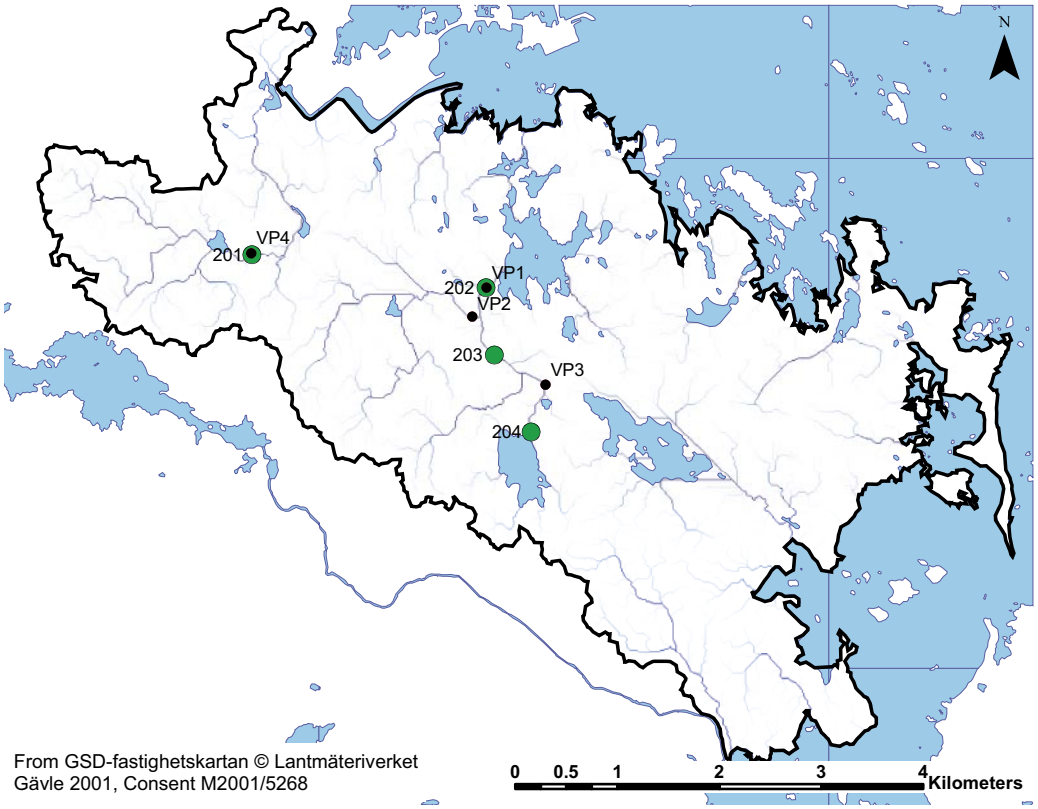

Figure 5-9. *Locations and IDs (VP1–VP4) of planned measurement stations considered in R-04-54, in comparison with updated locations and IDs of installed measurement stations (201–204) used here.*

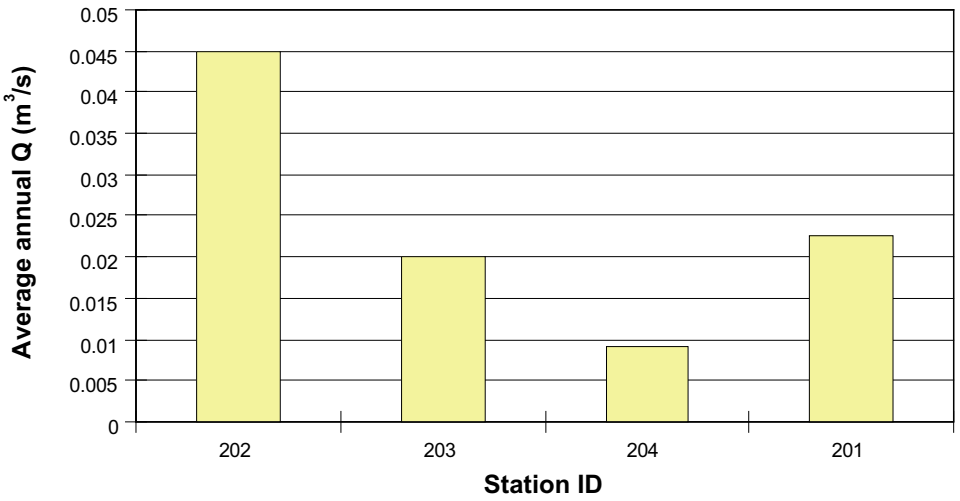

Figure 5-10. *Predicted average annual discharge Q at measurement stations 202, 203, 204 and 201.*

erably should be performed, we instead perform the calibration with the above results of the averaging procedure as target, considering these results to be our best representation of the long-term average hydrologic conditions. The goal of this exercise is then to adapt/calibrate method (ii) such that it can produce (in a single model run, i.e. without averaging of method (i) and method (ii) results) site-specific maps with local (cell by cell) evapotranspiration and precipitation surplus values that reproduce the target streamflow when used as input for the subsequent hydrological modelling step.

5.5 Calibrated stream flow estimates

The tabulated E_a-values used in method (ii) (see Table 3-1), originally determined by /Wendland 1992/, was recalibrated considering the Forsmark catchment using a single correction factor X^{cal}_{Ea} according to Equation (4) and the methodology outlined in Section 3.1. In Forsmark, the area-averaged precipitation was estimated to be equal to 667 mm×year^{-1} and the area-averaged evapotranspiration according to the (uncalibrated) method (ii) results was equal to 497 mm×year^{-1}, which implies a ratio between the cumulative precipitation and the cumulative method (ii) evapotranspiration ($\Sigma P/\Sigma E_a^{(ii)}$; see Equation (4)) of 1.34. Furthermore, the ratio r_q between the (assumed representative) target runoff (see discussion in Section 3.1) and the runoff predicted by method (ii) was equal to 1.33. Equation (4) then yields a calibration factor $X^{cal}_{Ea} = 0.89$. Multiplying all the data in Table 3-1 with this factor, we show in Table 5-1 the obtained calibrated method (ii) land use/soil cover E_a-values for Forsmark. The Forsmark E_a-values are slightly lower than the correspondingly calibrated values for Simpevarp (Table 7-1), which is consistent with the lower average temperatures of the more northern Forsmark catchment.

The Table 5-1 values were used in combination with E_a method (ii), instead of the values in Table 3-1. Each (pixel) value in the resulting, re-calculated, evapotranspiration map then differs by a factor 0.89 from the corresponding value shown in Figure 5-1b. Finally, this re-calculated map is used in a subsequent modelling step for producing calibrated stream flow estimates.

Here, we only show the calibrated results for average annual discharge Q at the planned measurement stations (Figure 5-11). However, all calibrated input and output results are available electronically according to Appendix 1. As pointed out in more detail previously (see, e.g. Section 3.1) the calibration procedure ensures that the overall discharge within the model area is equal to the (estimated and assumed representative) target discharge q_{est}. Notably, the distribution of discharge within the model area is not explicitly addressed in the calibration, minimizing the number of calibration parameters (to one, single calibration factor). Nevertheless, based on the Section 5.2 and R-04-54 finding that the two rather different E_a-methods (i) and (ii) yield the same relative flows among different catchment outlets (or measurement stations), we also expect that the calibrated model will yield a similar distribution of discharges at the measurement stations as our best estimate in Section 5.5 (Figure 5-10). Figure 5-11 shows that the calibration was successful in this respect, i.e. we could obtain, using one modelling step (based on E_a-method (ii)) and one calibration factor, results that are very similar to the ones shown in Figure 5-10.

Table 5-2. Calibrated method (ii) E_a-values considering the Forsmark catchment, using a single correction factor X_{cal}^{Ea} = 0.89 for adjusting the original values of Table 3-1, according to Equation (4) and the methodology outlined in Section 3.1.

Soil texture:	E_a(mm/year)	
Land cover:	Forest	Other land cover
Very fine	506	488
Fine	488	417
Medium fine	470	375
Medium	422	333
Coarse	399	288
Peat	n.a.	462
Water	n.a.	533

n.a. = not applicable.

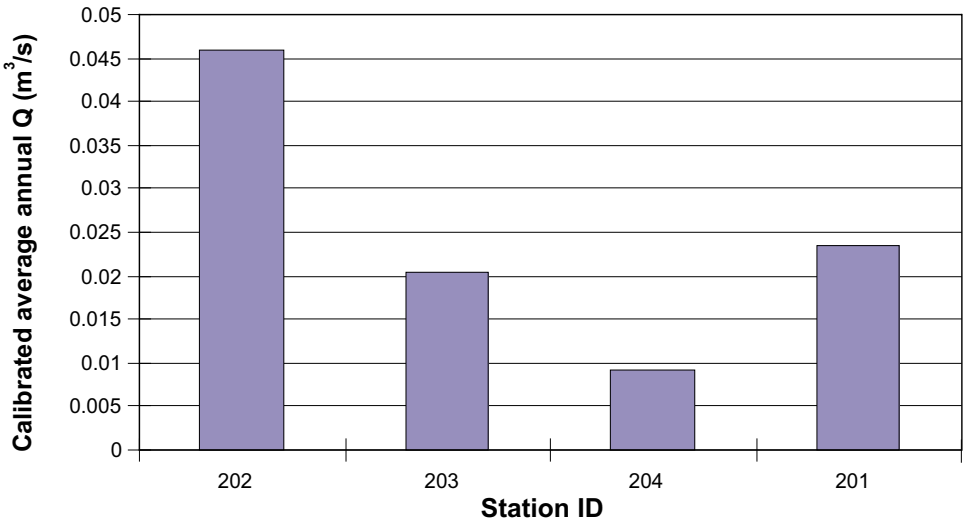

Figure 5-11. *Calibrated average annual discharge Q at Forsmark measurement stations 202, 203, 204 and 201, showing results very similar to Figure 5-10.*

6 Application Simpevarp: The catchment and input data

6.1 Model area, digital elevation model and streams

The location of the study area is shown in Figure 6-1. It extends all the way to the coast, including very small coastal sub-catchments (limited by the grid resolution of 10×10 m). The total number of coastal catchment outlets within the study area is 6,844. Figure 6-2 shows more details, such as the catchment boundary (yielding a model area of 127.7 km^2), streams and the location ID of the 13 outlets with the highest flow values, representing together approximately 80% of the total annual average discharge Q_{TOT}, with local stream discharge $Q_i > 0.01Q_{TOT}$ at each location. For comparison, we used the same criteria for identifying the most important outlets in Forsmark, resulting there in a total of 10 outlets (Section 4.1).

The original version 1.2 digital elevation model for the site investigation programme in Oskarshamn /Brydsten and Södergren 2005/ was changed according to the summary in Appendix 1 and the previous description in R-04-54 (except for the described manipulation regarding the catchment boundary, which here is given through the digital elevation model). Due to the specific account for river locations in these changes, the here derived catchment boundaries (Figure 6-2) are in most cases consistent with the field-controlled boundaries reported by /Lindborg 2005/. This is for instance the case for the relatively long border between catchments 5 and 10, using the same sub-catchment numbering as in Figure 3-44, p 88 in /Lindborg 2005/ (although not explicitly shown in Figure 6-2).

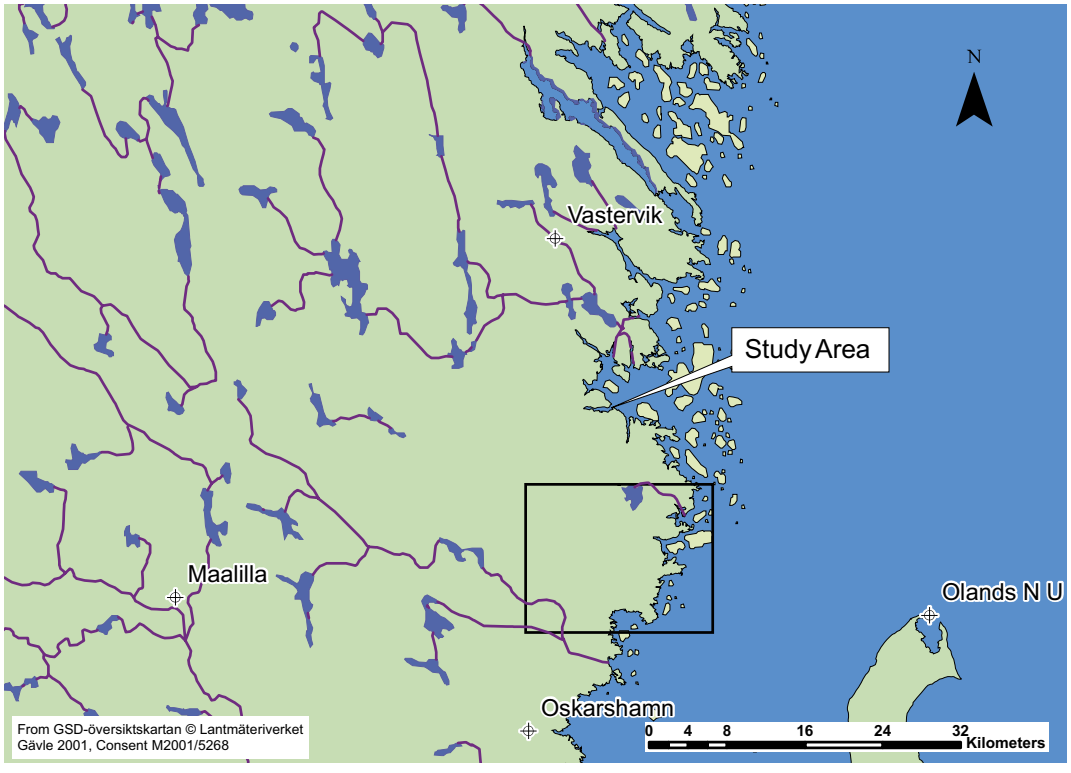

Figure 6-1. *Location of the study area and nearby SMHI meteorological stations.*

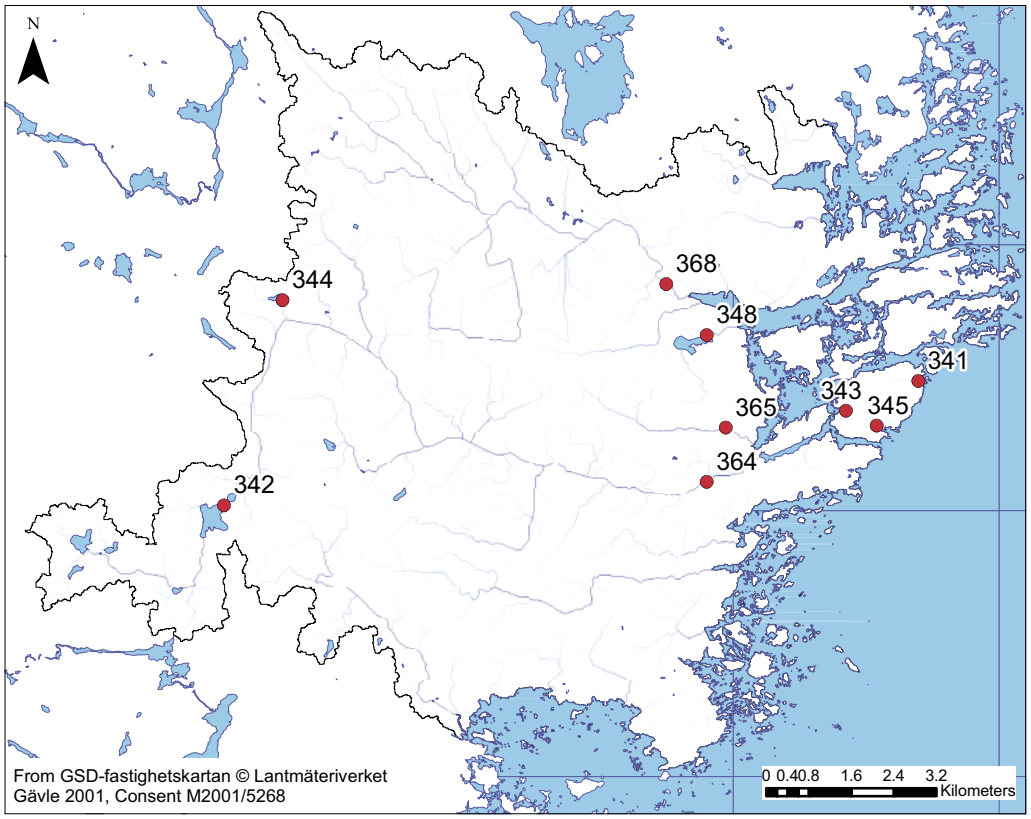

Figure 6-2. *Location of catchment boundary, streams (both determined on the basis of the DEM after, e.g. lowering the elevations at known stream locations by 3 m) and hydrological measurement stations*

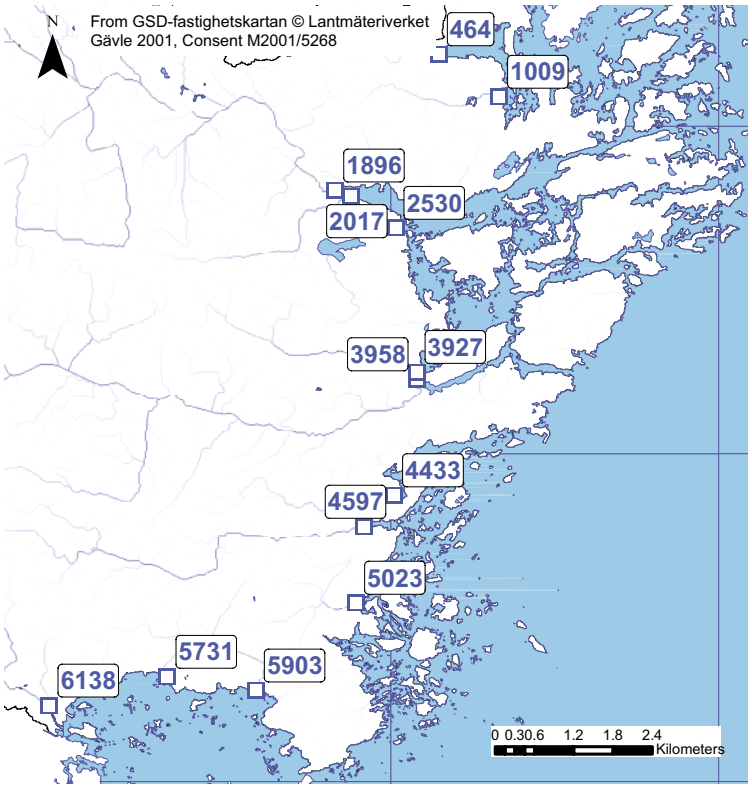

Figure 6-3. *Location of the stream outlets for the 13 largest sub-catchments in the present modelling, contributing together to approximately 80% of the total coastal discharge from the model area.*

However, the outlet point location of catchment 17 (number 4,597 in Figure 6-3) differs from the previously reported one, with its here determined location being the same as the outlet location of catchment 13 in /Lindborg 2005/. This is because of the river stretches in the used ESRI input file "hydrografi.shp " are connected in this way (this affects local predictions so it should be checked), rather than in the way implied by the field-controlled results of /Lindborg 2005/. In addition, Figure 6-2 shows the location of hydrological measurement stations, for which we predict the stream flows in Section 7-4.

6.2 Precipitation

Annual and seasonal precipitation data were taken from three SMHI meteorological stations (Målilla, Oskarshamn and Ölands N Udde; data summarised in /Larsson-McCann et al. 2002b/). We extended the point data throughout the model area by conducting spline interpolation and extrapolation (see also Appendix 1), resulting in the map of Figure 6-4. Since no precipitation data was reported in /Larsson-McCann et al. 2002b/ for the regions north of the model area, we instead used extrapolation of /Larsson-McCann et al. 2002b/ data to cover this northernmost region. A possible consequence of this is that the northernmost precipitation is somewhat underestimated, since the island station at Ölands N Udde (Figure 6-1), showing lower precipitation than the land-based stations, becomes more influential on this region.

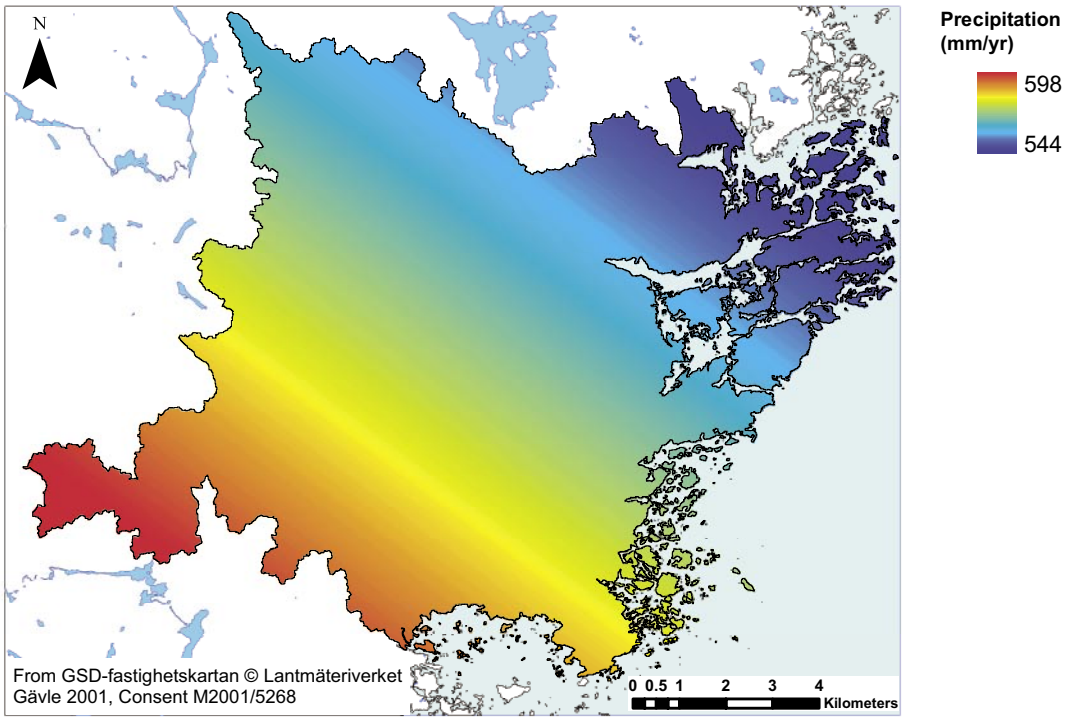

Figure 6-4. *Interpolated and extrapolated annual average precipitation P (mm/year) for the considered Simpevarp area, with the maximum and minimum P within the area indicated in the legend.*

6.3 Temperature

Temperatures were calculated on the basis of data (summarised in /Larsson-McCann et al. 2002b/) from three SMHI meteorological stations (Målilla, Oskarshamn and Ölands N Udde; Figure 6-5 and Appendix 1) complemented with data from a fourth station in Västervik from the SMHI journal "Väder och vatten".

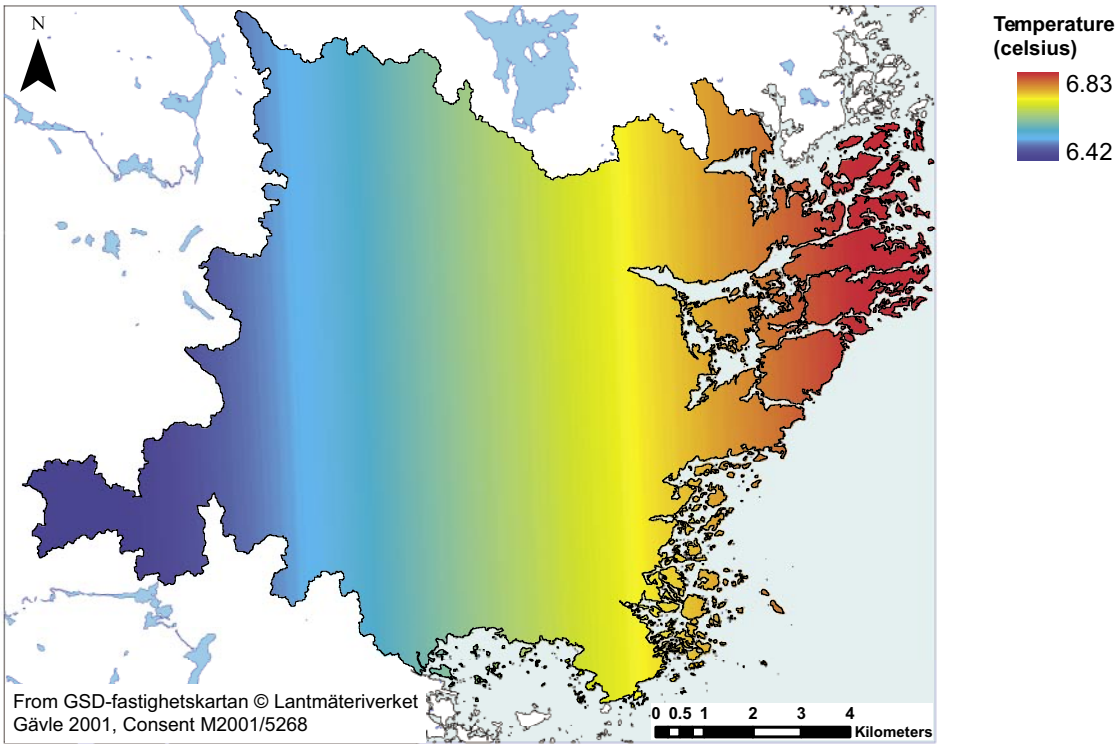

***Figure 6-5**. Interpolated annual average temperature T (°C) for the Simpevarp area, with the maximum and minimum T within the area indicated in the legend.*

6.4 Soil data

The soil input data was given by the SGU map series “Jordartsinformation i serie Ae” and the SGU classification code “Klartextbeskrivning J123” was used. The data was provided to us in processed form by SKB in the ArcGIS shape file SDEADM_SGU_SM_GEO_2502.shp. The translation of the soil classes into the soil texture classes needed as input for the PCRaster-POLFLOW model is shown in Table 6-1. The resulting soil texture map, used as input for the updated model, is shown in Figure 6-6. We note that detailed data for a region in the upstream part of the catchment are missing, because SKB does not have access to this region. We derived uniform properties for this region, based on the prevailing properties of the surroundings, resulting in a 100% green field in the left part of Figure 6-6.

Table 6-1. Translation of the soil categories in the SGU coding “J123” to the six soil texture classes and an additional water class required by the empirical relations used in this work, considering the Simpevarp area.

Soil category given in the SGU classification “J123”	Class	PCRaster Code
Rock, unspecified	Coarse	1
Soil – boulder	Coarse	1
Coarse silt – boulder	Coarse	1
Surge sediment, gravel	Coarse	1
Surge sediment, gravel with thin surface layer of peat	Coarse	1
Surge sediment, sand	Coarse	1
Surge sediment, sand with thin surface peat layer	Coarse	1
Surge sediment, stone – boulder	Coarse	1
Bedrock	Coarse	1
Sandy till	Medium	2
Sandy till with thin surface peat layer	Medium	2
Surge sediment, clay – gravel (postglacial, more recent)	Medium	2
Fillings on unknown subsurface	Medium fine	3
Till	Medium fine	3
Glacial silt	Fine	4
Clay – silt (glacial and postglacial)	Fine	4
Glacial clay, unspecified	Very fine	5
Glacial clay, unspecified with thin surface peat layer	Very fine	5
Gyttja	Very fine	5
Clayey gyttja – gyttja clay	Very fine	5
Clayey gyttja – gyttja clay with thin surface peat layer	Very fine	5
Peat	Peat	6
Fen peat	Peat	6
Bog peat	Peat	6
Water	Water	7

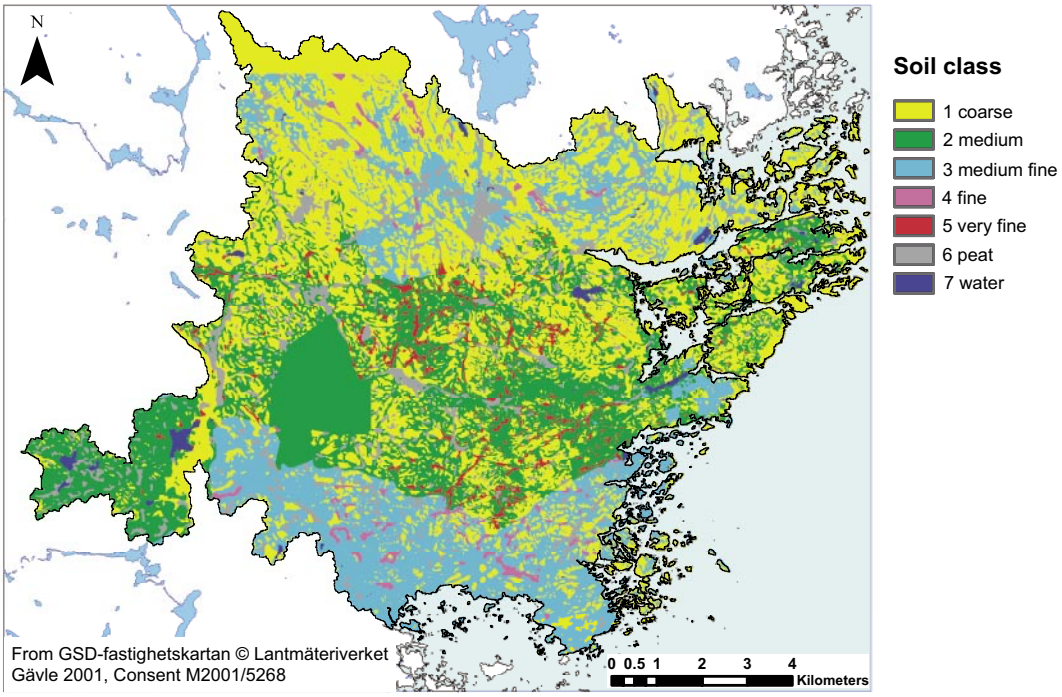

Figure 6-6. *The soil texture map for Simpevarp, used as input for the hydrological modelling. Derived on basis of the SGU soil type map "Jordartsinformation i serie Ae" translated as in Table 6-1.*

6.5 Land cover (vegetation) data

Updated groundlayer and vegetation data was provided to us in processed form by SKB in the ArcGIS shape file SDEADM_SWP_OSK_BIO_1251.shp. The altogether 36 original data classes (see /Boresjö Bronge and Wester 2003/ for details) were reduced according to Table 6-2 to the five land cover classes used in the present PCRaster-POLFLOW model. The resulting land cover map, used as input for the model, is shown in Figure 6-7.

Table 6-2. Translation of 36 original vegetation and groundlayer classes to 5 new land cover classes required by the empirical relations used in this work, considering the Simpevarp area.

Original vegetation class	Land cover class (translated)	PCRaster code
Coastal rocks	Built-up	1
Industry	Built-up	1
Lowrise house	Built-up	1
Other hard surfaces	Built-up	1
Old clear-cut, young spruce	Open land	2
Old clear-cut, young pine	Open land	2
Old clear-cut, unspecified conifer	Open land	2
Old clear-cut, birch thicket	Open land	2
Old clear-cut, birch thicket/meadow type	Open land	2
New clear-cut	Open land	2
Arable land	Open land	2
Other open land (pastures and meadows)	Open land	2

Original vegetation class	Land cover class (translated)	PCRaster code
Sand or stone pit	Open land	2
Holiday house	Open land	2
Old spruce-dominated forest, mesic-wet types	Forest	3
Young spruce-dominated forest, mesic-wet types	Forest	3
Old pine-dominated forest, mesic-wet types	Forest	3
Young pine-dominated forest, mesic-wet types	Forest	3
Dry pine forest on acid rocks	Forest	3
Coastal deciduous forest (birch/oak) or thicket	Forest	3
Birch forest or oak/maple mixed with conifers	Forest	3
Oak-dominated deciduous forest	Forest	3
Mixed forest (conifers/deciduous)	Forest	3
Forested wetland, pine-dominated	Forest	4
Forested wetland, birch-dominated	Forest	4
Open wetland, hummock mire	Wetland	4
Open wetland, poor lawn mire	Wetland	4
Open wetland, lush lawn mire	Wetland	4
Open wetland, very lush lawn mire, with tall her	Wetland	4
Open wetland, very lush lawn mire, with willow	Wetland	4
Open wetland, poor carpet mire, Sphagnum-dominat	Wetland	4
Open wetland, lush swamp fen	Wetland	4
Open wetland, lush swamp fen, reed-dominated	Wetland	4
Open wetland, reed-dominated, poorer or wetter	Wetland	4
Floating mats/macrophytes	Wetland	4
Water	Water	5

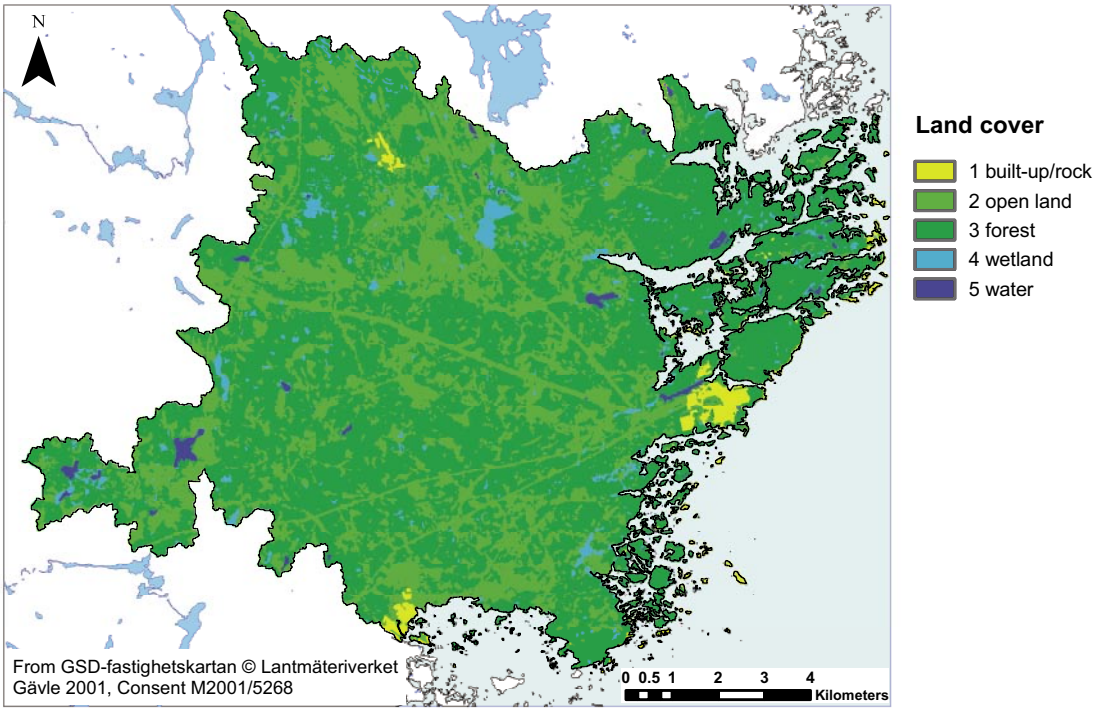

Figure 6-7. *The land cover map for Simpevarp, used as input for the hydrological modelling. The map was derived following the translation of Table 6-2.*

7 Application Simpevarp: Results

7.1 Precipitation surplus and runoff

Figures 7-1 (a) and (b) show estimates of evapotranspiration E_a in the Simpevarp area using methods (i) and (ii), respectively (see Section 5.1 in R-04-54 for a detailed descriptions of the methods). As for the Forsmark application (see Chapter 5 in this report and R-04-54), method (ii) (Figure 7-1 (b)) implies a higher degree of local variation, because the underlying local soil and vegetation maps (Figures 6-6 and 6-7) are much more detailed than the temperature map (Figure 6-5), which is based on only four measurement stations. There is some degree of local variation also in the method (i)-prediction of E_a (Figure 7-1(a)), however, because the illustration resolution is, for direct comparison purposes, scaled the same in both Figures 7-1(a) and 7-1(b), this smaller variation is not clearly visible in Figure 7-1(a). Again, as for the Forsmark application, method (ii) generally predicts higher values of E_a than method (i).

Figures 7-2 (a) and (b) show the local precipitation surplus (PS), calculated through Equation (1) in R-04-54, using evapotranspiration methods (i) and (ii), respectively. Method (ii) generally predicts lower PS (which also equals the total locally created runoff, R) because its E_a estimates are generally higher (Figure 7-1). The estimated local groundwater recharge index is shown in Figure 7-3.

Averaging the local R values shown in Figure 7-4 over the entire model area, we obtain the normalised runoff values presented in Table 7-1. For comparison, the regional average runoff in the area was estimated independently by /Larsson-McCann et al. 2002b/ to 5.7 $ls^{-1}km^{-2}$ (which corresponds to 180 mm/year). Furthermore, for one of the sub-catchments within the here considered area, the modelled specific runoff with MIKE SHE was 4.9 $ls^{-1}km^{-2}$ /Lindborg 2005/. Table 7-1 shows that these independent estimates are within the herein calculated runoff range 3.97 l/s/km^2 (method (ii)) to 5.89 l/s/km^2 (method (i)). The average calculated runoff by the two methods of 4.93 l/s/km^2 is close to the above-mentioned independently estimated values; this is consistent with the experience from the Forsmark application (Chapter 5 in this report and R-04-54) as well as previous experience from the Norrström drainage basin using PCRaster-POLFLOW /Greffe 2003/.

Table 7-1. Modelled area-averaged (i.e. specific) runoff in the Simpevarp catchment using different evapotranspiration estimation methods (i) and (ii).

Specific runoff	Prediction method	Main input variable(s)
5.89 l/s/km^2	Method (i)	Temperature
3.97 l/s/km^2 l/s/km^2	Method (ii)	Soil type and land cover
Average: 4.93 l/s/km^2	–	–

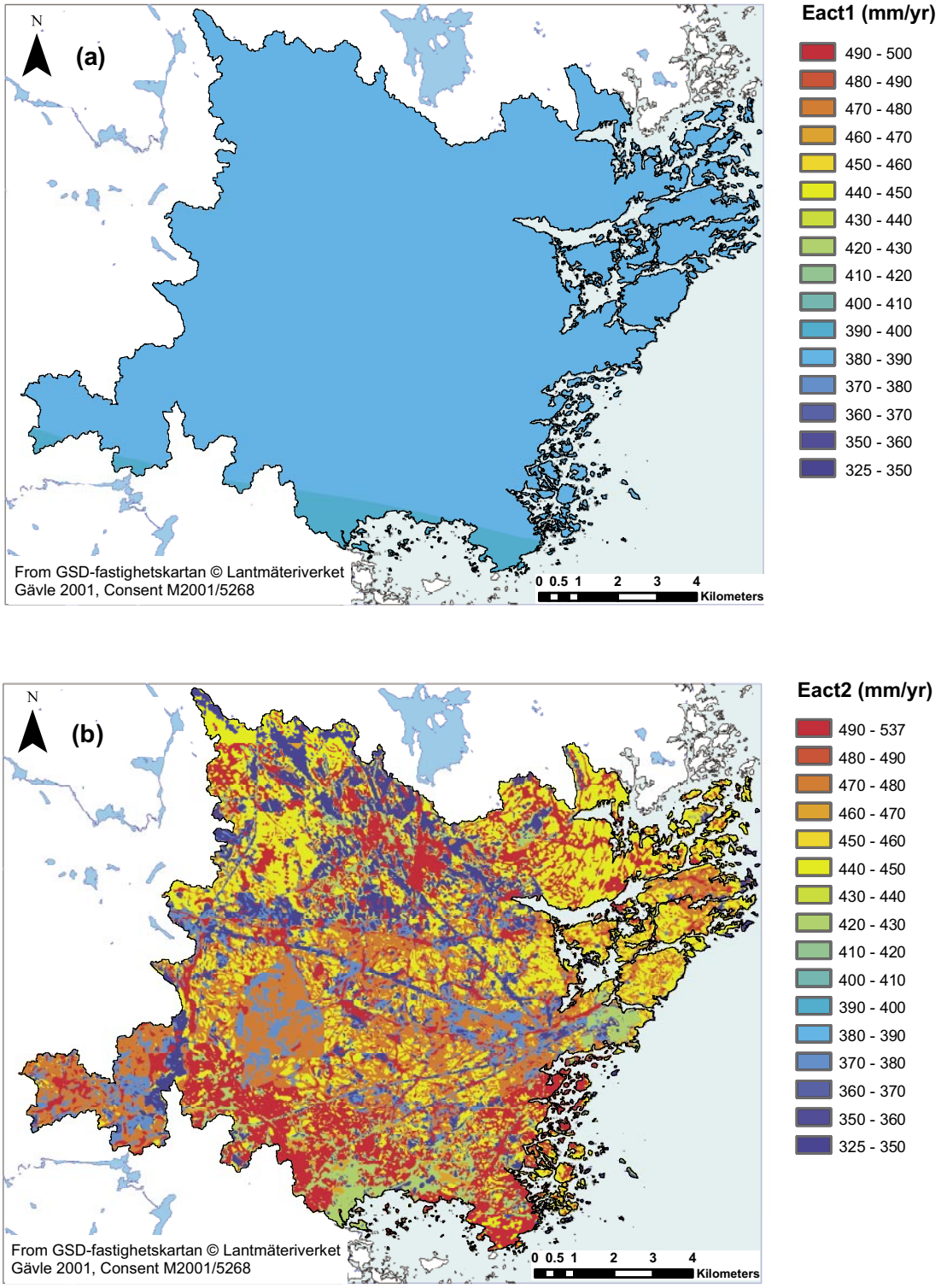

Figure 7-1. *Calculated evapotranspiration E_a (in mm/year), using (a) method (i) and (b) method (ii).*

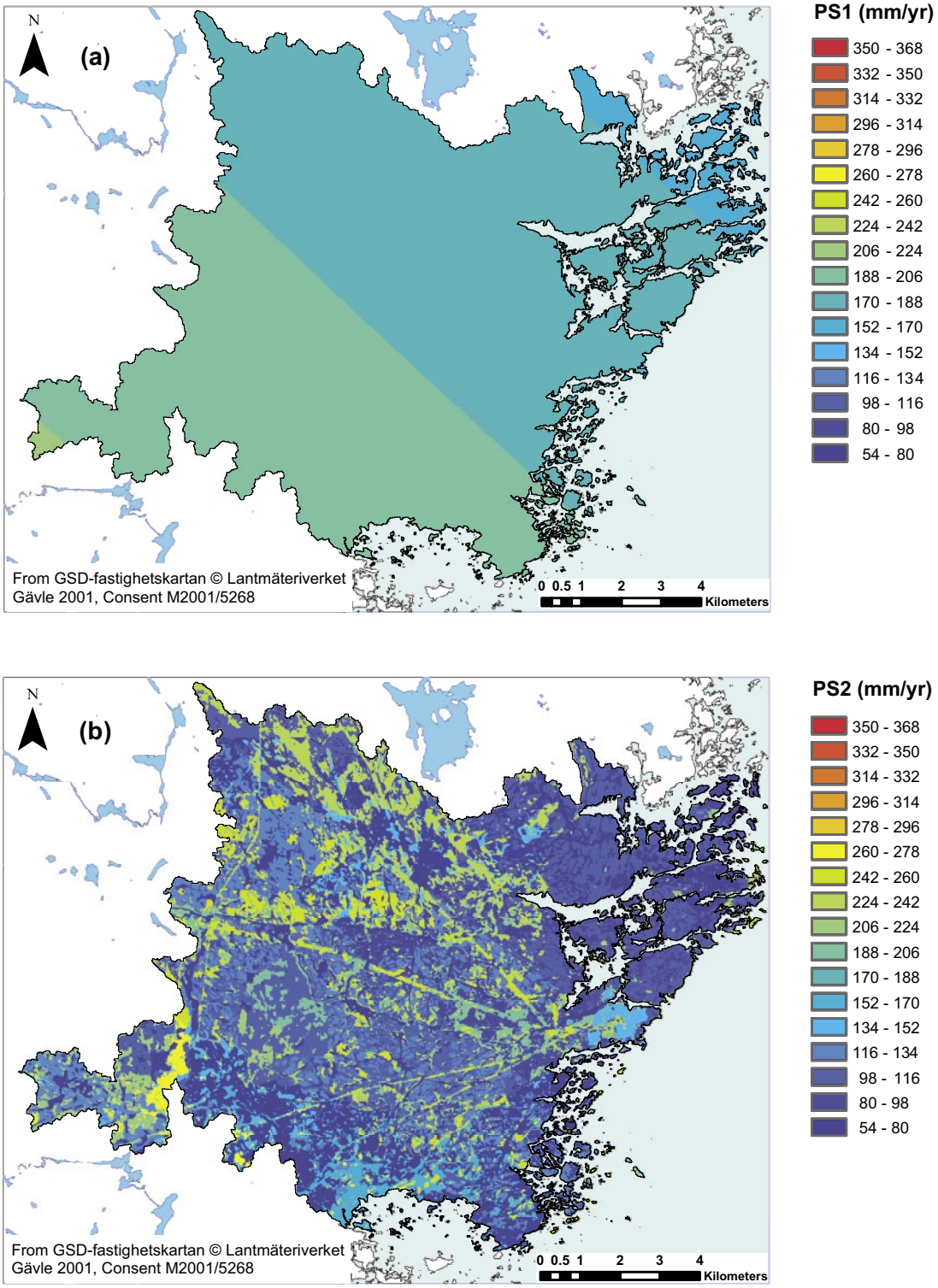

Figure 7-2. *Calculated local precipitation surplus, PS, (in mm/year), using (a) method (i) and (b) method (ii).*

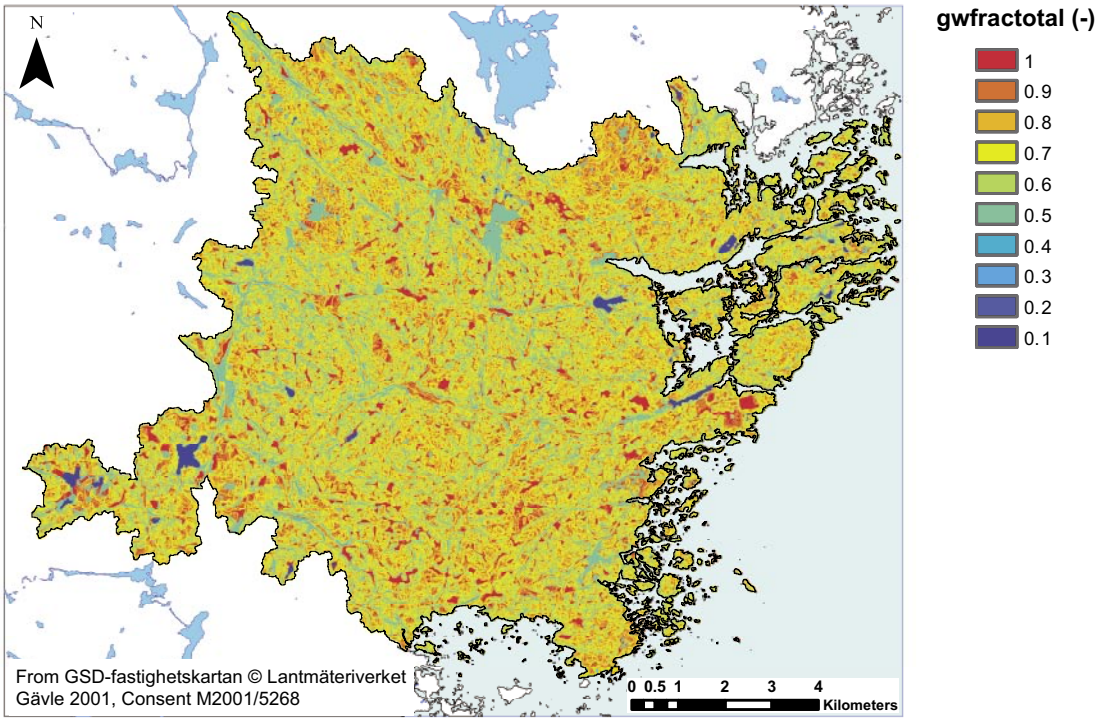

Figure 7-3. *The calculated groundwater recharge index, f_{gw}.*

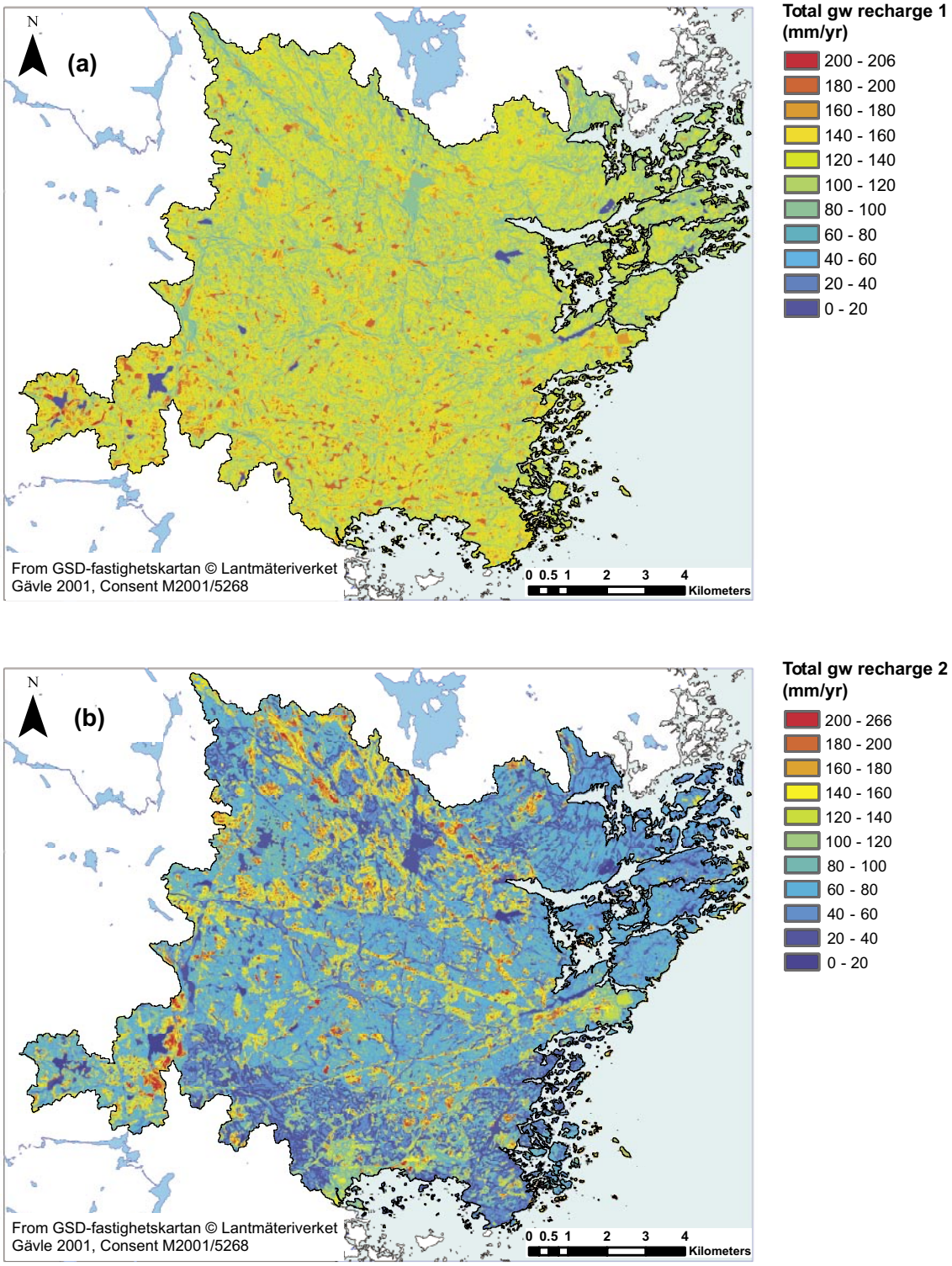

Figure 7-4. *The calculated local groundwater recharge, GW (in mm/year), using (a) method (i) and (b) method (ii).*

7.2 Streamflow distribution among different coastal outlets

Figure 7-5 shows the calculated coastal streamflow, Q (Equation (6) in R-04-54) for the top 13 outlets with regard to high Q- values (see Figure 6-3 for their location), out of the 6,844 outlets (on the 10×10 m scale). Whereas the 13 outlets together contribute to 80% of the total coastal discharge from the modelled area as previously mentioned, two of the outlets, number 3,958 and 1,896 together contribute to more than 50% of the total discharge. On the other hand, in order to cover 90% of the total coastal discharge, approximately 80 outlets need to be considered. Figure 7-6 shows a result for Simpevarp that is similar to the one previously presented for Forsmark, namely that E_a-methods (i) and (ii) yield approximately the same *relative* flows among the selected outlets.

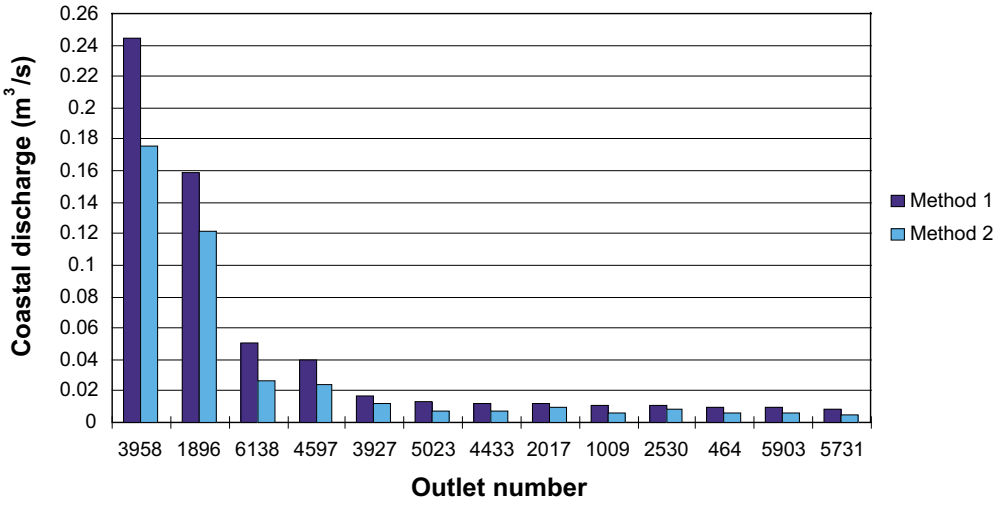

Figure 7-5. *Estimated coastal stream discharge Q (Equation (6) in R-04-54) through the 13 largest coastal stream outlets within the Simpevarp area (contributing to 80% of the total discharge from the area; see Figure 6-3 for their location) for E_a-method (i) (dark blue bars) and E_a-method (ii) (light blue bars).*

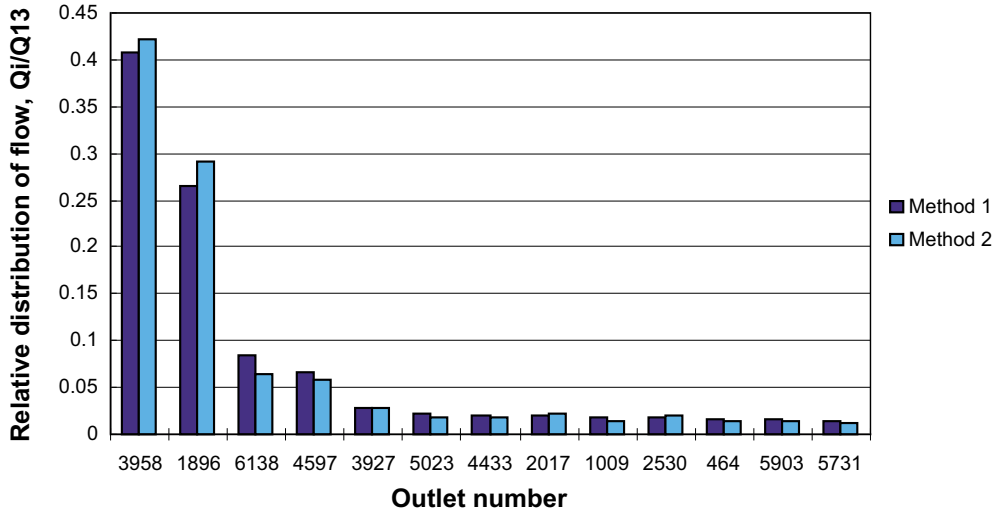

Figure 7-6. *Relative distribution Q_i/Q_{13} of the sum of flow for the 13 selected Simpevarp outlets Q_{13} among these outlets i (i = 1 to 13), for E_a-method (i) (dark blue bars) and E_a-method (ii) (light blue bars).*

Hence, the updated results for Forsmark, as well as the new Simpevarp results support the conclusion in R-04-54 that the differences between the methods mainly regard their mean, or total, outflow estimates. Therefore, we could here develop a calibration procedure regarding E_a method (ii), using one site-specific calibration factor that adjusts for systematic deviations in its results.

7.3 Average seasonal stream flow in coastal outlets

The estimated average seasonal coastal discharge (see Section 5.3 for details) for the Simpevarp area is shown in Figure 7-7, accounting for average differences in precipitation and evapotranspiration between the seasons. However, whereas site-specific precipitation data was used, the relative evapotranspiration differences between the seasons were obtained from an SMHI study (see R-05-54 for details). The predicted average discharge within the summer season (dark blue bars) is approximately one quarter of that in the winter season (light blue bars), which is considerably less than the Forsmark prediction (Section 5.3).

Regarding the absolute values, we note that method (i) appears to generally over-predict the average annual precipitation surplus and runoff. We also note that the Simpevarp results on the relative distribution of flow among the different outlets (Figure 7-8) provides further support for the conclusion made in Section 5.3 that the calibration methodology outlined in Section 3.1 may be relevant also for estimation of seasonal conditions (in larger catchments). The reason is that results show the same relative distribution of flow among the 13 selected outlets during both the winter season and the summer season (Figure 7-8), such that one single calibration factor would be sufficient to correct for systematic bias in all 13 selected coastal outlets.

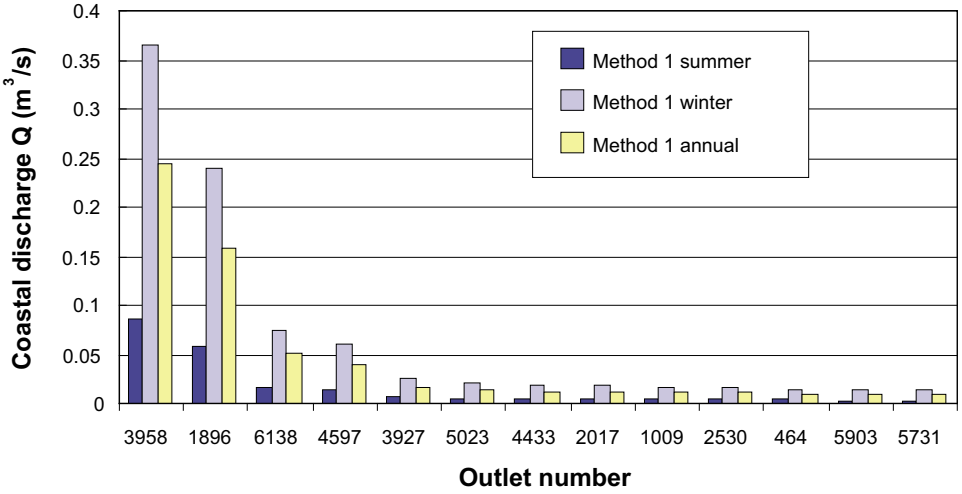

Figure 7-7. *Average, seasonal coastal discharge in summer (dark blue bars) and winter (light blue bars), using method (i) (for the 13 outlets with largest discharge). For comparison, the light yellow bars show the annual average discharge values predicted by method (i).*

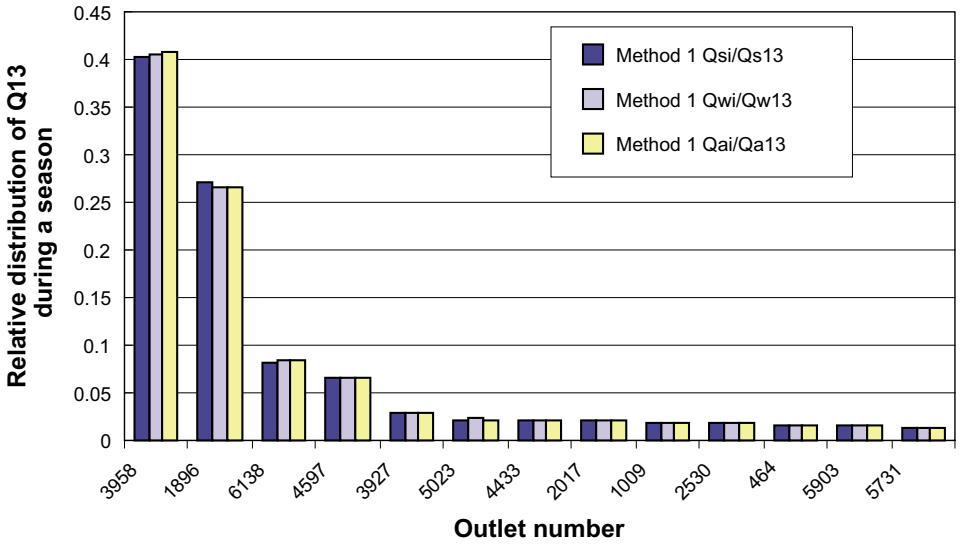

Figure 7-8. *Relative distribution of total average seasonal discharge Q13 among the 13 largest coastal outlets. The blue bars show results for the summer season (indicated by index s) for each outlet i (Qsi/Qs13, where Qsi is the flow at each coastal outlet and Qs13 is the sum of flow from the 13 considered outlets), the grey bars show results for the winter season (indicated by index w; Qwi/Qw13), and the light yellow bars show results for the average annual discharge (index a; Qai/Qa13).*

7.4 Stream flow in measurement stations

The location of streamflow measurement stations within the modelled Simpevarp catchment is indicated in Figure 6-2. Figure 7-9 shows our expected best estimate of the average annual discharge Q at these measurement stations, which is based on the averaging of the flow results from methods (i) and (ii), with basic results of estimation methods (i) and (ii) being listed in Table 7-1. As for the Forsmark case, we will in the following section use a (re-) calibration procedure considering only method (ii), and produce results similar to the above using one model run only.

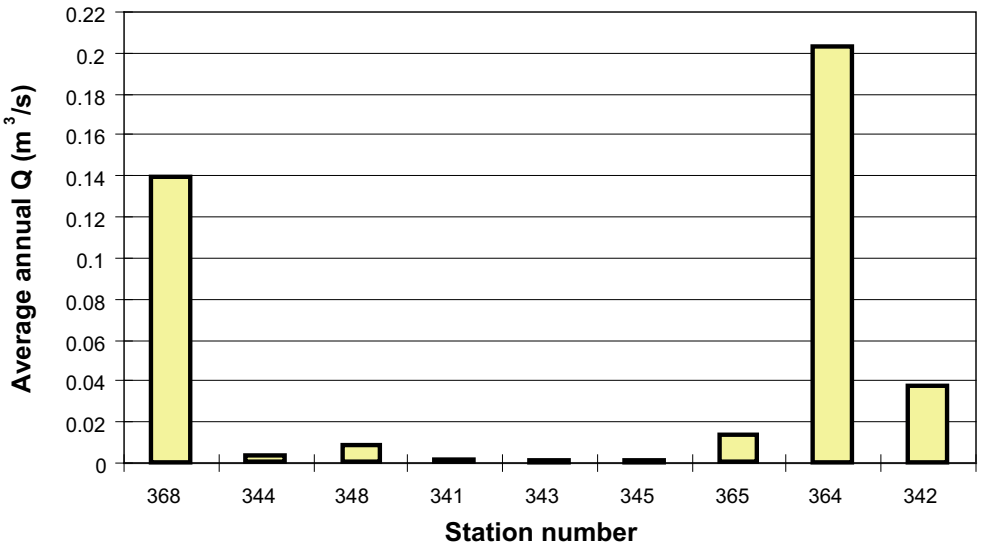

Figure 7-9. *Predicted average annual discharge Q at Simpevarp measurement stations, see also Table 7-1.*

Table 7-2. Expected best estimate of average annual discharge Q (also shown in Figure 7-9), compared to average annual discharge for E_a-method (i), average annual discharge for E_a-method (ii), and average seasonal relative to average annual discharge during summer and winter seasons.

		Measurement station (Figure 6-2)								
	Unit	368	344	348	341	343	345	365	364	342
Annual, average discharge *q* (average value of method (i) and (ii), shown in **Figure 7-9**)	(m^3/s)	**0.139**	**2.6 ×10^{-3}**	**8.4 ×10^{-3}**	**1.2 ×10^{-3}**	**5.1 ×10^{-4}**	**8.0 ×10^{-4}**	**0.013**	**0.203**	**0.038**
Annual, average *q*, *method (i)*	(m^3/s)	0.158	3.1 ×10^{-3}	9.7 ×10^{-3}	1.6 ×10^{-3}	6.4 ×10^{-4}	1.0 ×10^{-3}	0.015	0.237	0.043
Annual, average *q*, *method (ii)*	(m^3/s)	0.120	2.0 ×10^{-3}	7.1 ×10^{-3}	8.6 ×10^{-4}	3.8 ×10^{-4}	6.1 ×10^{-4}	0.011	0.169	0.031
Average seasonal relative to average annual *q* during **summer** season (June to Sept)	(–)	**0.36**	**0.35**	**0.36**	**0.37**	**0.37**	**0.37**	**0.36**	**0.35**	**0.34**
Average seasonal relative to average annual *q* during **winter** season (Oct to May)	(–)	**1.51**	**1.48**	**1.53**	**1.55**	**1.55**	**1.55**	**1.52**	**1.49**	**1.46**

Regarding the prediction of seasonal, average discharge values, we used the temperature-based method (i) for obtaining results for summer and winter conditions. The results are listed in Table 7-2, and expressed in percent of the annual, average discharge. For instance, the value of about 36% for the summer season hence implies that the streamflow during an average summer day (between June and September) is expected to be 36% of the annual, average streamflow. This is lower than the corresponding result for the Forsmark catchment of about 53% (R-04-54).

7.5 Calibrated stream flow estimates

In analogy with the modelling of the Forsmark catchment (Section 5.5), the tabulated E_a-values used in method (ii) (see Table 3-1), originally determined by /Wendland 1992/, was recalibrated considering the Simpevarp catchment using a single correction factor X^{cal}_{Ea} according to Equation (4) and the methodology outlined in Section 3.1. In Simpevarp, the area-averaged precipitation was estimated to be equal to 574 mm×year^{-1} and the area-averaged evapotranspiration according to the (uncalibrated) method (ii) results was equal to 448 mm×year^{-1}, which implies a ratio between the cumulative precipitation and the cumulative method (ii) evapotranspiration ($\Sigma P/\Sigma E_a^{(ii)}$; see Equation (4)) of 1.28. Furthermore, the ratio r_q between the here considered correct runoff (see discussion in Section 3.1) and the runoff predicted by method (ii) was equal to 1.24. Equation (4) then yields a calibration factor $X^{cal}_{Ea} = 0.93$. Multiplying all the data in Table 3-1 with this factor, we show in Table 7-1 the obtained calibrated method (ii) land use/soil cover E_a-values for Simpevarp. The Simpevarp E_a-values are slightly higher than the correspondingly calibrated values for Forsmark (Table 5-1), which is consistent with the higher average temperatures of the more southern Simpevarp area.

As for the Forsmark case (Section 5.5), the Table 7-3 values were used in combination with E_a method (ii), such that each (pixel) value in the resulting, re-calculated, evapotranspiration map differed by a factor 0. 93 from the corresponding value shown in Figure 7-1b. This re-calculated map was used in a subsequent modelling step for producing calibrated stream flow estimates.

All calibrated input and output results are available electronically according to Appendix 1. Figure 7-10 shows that the calibration was successful, i.e. we could obtain through one modelling step (using E_a-method (ii)), results that are approximately the same as the ones shown in Figure 7-9.

Table 7-3. Calibrated method (ii) E_a-values considering the Simpevarp catchment, using a single correction factor X_{cal}^{Ea} = 0.93 for adjusting the original values of Table 3-1, according to Equation (4) and the methodology outlined in Section 3.1.

Soil texture:	E_a(mm/year)	
Land cover:	Forest	Other land cover
Very fine	531	512
Fine	512	438
Medium fine	493	394
Medium	442	349
Coarse	419	303
Peat	n.a.	484
Water	n.a.	559

n.a. = not applicable.

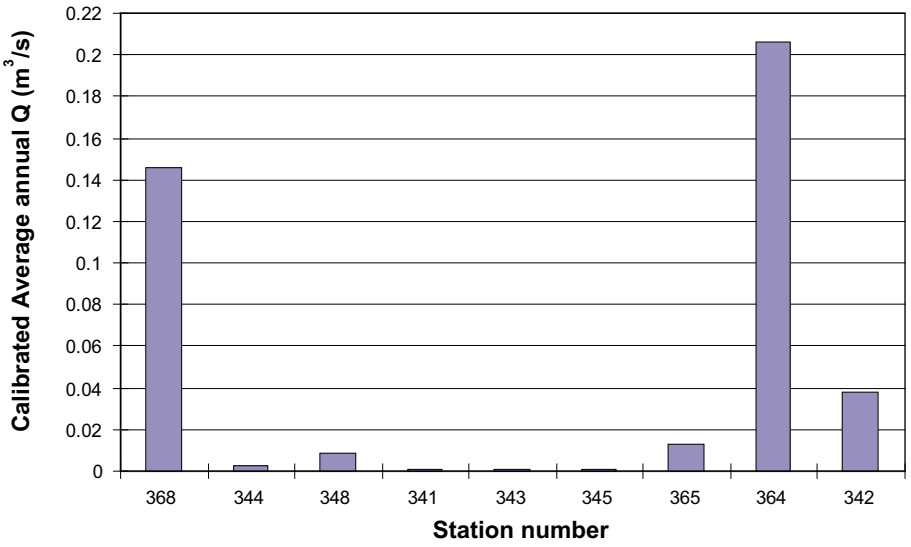

Figure 7-10. *Calibrated average annual discharge Q at measurement stations in Simpevarp, showing results identical to Figure 7-9.*

8 Conclusion summary

We presented new hydrological modelling results for the Simpevarp area and updated the Forsmark modelling results (originally reported in R-04-54), using SKB v 1.2-data. The model areas were extended all the way to the coastline, enabling consideration of interactions with seawater in future studies. Furthermore, we delivered results for comparison with data that currently are collected through the on-going measurements at the hydrological stations in Forsmark and Simpevarp.

- It was shown through the updated Forsmark site-assessment, as well as the new Simpevarp site-assessment, that the PCRaster-POLFLOW model can yield results that are consistent with available, independent (regional) hydrologic runoff data, through averaging of uncalibrated results using two different evapotranspiration estimation methods, as previously indicated in R-04-54.
- The choice of evapotranspiration estimation method can influence the predictions to a relatively large degree. In addition to the two methods discussed in detail here, the PCRaster-POLFLOW framework can be used in combination with other evapotranspiration methods or quantifications, e.g. remote sensing models (see R-04-54) or data from the Coup Model.
- Furthermore, Forsmark and Simpevarp results support the conclusion in R-04-54 that the different results produced by the two tested evapotranspiration methods (i) and (ii) mainly regard the prediction of mean, or total, outflow. Therefore, we could here develop a calibration procedure regarding method (ii), using one site-specific calibration factor that adjusts for systematic deviations in its results.
- Using the calibrated Forsmark and Simpevarp models, we could through a single modelling step (using E_a-method (ii)), produce results that were consistent with regional estimates of specific runoff.
- The uncalibrated method (ii) evapotranspiration values (originally developed for German conditions, taking into explicit account the soil type and land cover) were lowered slightly more in the Forsmark calibration than in the Simpevarp calibration, which is consistent with the lower average temperatures of the more northern Forsmark catchment.
- A comparison between Forsmark and Simpevarp results furthermore shows that
  - 10 sub-catchments contribute to 80% of the annual, average coastal discharge in the modelled Forsmark area, with each individual sub-catchment contributing to more than 1% of this total discharge; the corresponding number of sub-catchments for the Simpevarp area is 13.
  - The variation in average seasonal discharge is predicted to be larger for the Simpevarp area than for the Forsmark area, with the considered winter-season being an 8-month period between 1st of October and 31st of May, and the summer season being a 4-month period between 1st of June and 30th of September.

References

Boresjö Bronge L, Wester K, 2003. *Vegetation mapping with satellite data of the Forsmark, Tierp and Oskarshamn regions*. SKB P-03-83. Svensk Kärnbränslehantering AB.

Brydsten L, Strömgren M, 2004. *Digital elevation models for site investigation programme in Forsmark*. SKB R-04-70. Svensk Kärnbränslehantering AB.

Brydsten L, Strömgren M, 2005. *Digital elevation models for site investigation programme in Oskarshamn*. SKB R-05-38. Svensk Kärnbränslehantering AB.

Darracq A, 2003. *Dynamic characterization of nutrient transport in the Norrström drainage basin.* TRITA-LWR Master Thesis, Dept. of Land and Water Resources Engineering, KTH, Stockholm.

Darracq A, Destouni G, 2005. In-stream nitrogen attenuation: model artifacts and management implications for coastal nitrogen impacts. *Environmental Science & Technology*, 39, 3716–3722.

Darracq A, Greffe F, Hannerz F, Destouni G, Cvetkovic V, 2005. Nutrient transport scenarios in a changing Stockholm and Mälaren valley region, Sweden. *Water Science & Technology,* 51, 31–38.

De Wit M J M, 1999. *Nutrient fluxes in the Rhine and Elbe basins*. Ph.D. Thesis, Utrecht University, *NGS Publication* 259, 163 pp.

De Wit M J M, 2001. Nutrient fluxes at the river basin scale. I: the PolFlow model. *Hydrological Processes*, 15. 743–759.

Greffe F, 2003. *Material transport in the Norrström drainage basin: Integrating GIS and hydrological process modeling.* TRITA-LWR Master Thesis, Dept. of Land and Water Resources Engineering, KTH, Stockholm.

Jarsjö J, Shibuo Y, Destouni G, 2004. *Using the PCRaster-POLFLOW approach to GIS-based modelling of coupled groundwater -surface water hydrology in the Forsmark area.* SKB R-04-54. Svensk Kärnbränslehantering AB.

Langbein W B, 1949. *Annual runoff in the United States.* U.S. Geological Survey Circular 52, U.S. Dept. of the Interior: Washington D.C.

Larsson-McCann S, Karlsson A, Nord M, Sjögren J, Johansson L, Ivarsson M, Kindell S, **2002a.** *Meteorological, hydrological and oceanographical data for the site investigation program in the communities of Östhammar and Tierp in the northern part of Uppland*, SKB TR-02-02. Svensk Kärnbränslehantering AB.

Larsson-McCann S, Karlsson A, Nord M, Sjögren J, Johansson L, Ivarsson M, Kindell S, **2002b.** *Meteorological, hydrological and oceanographical data for the site investigation program in the community of Oskarshamn*, SKB TR-02-03. Svensk Kärnbränslehantering AB.

Lindborg (Ed.), 2005. *Description of surface systems. Preliminary site description Simpevarp sub area – Version 1.2.* SKB R-05-01. Svensk Kärnbränslehantering AB.

Meinardi C, Beusen A, Bollen M, Klepper O, 1994. Vulnerability to diffuse pollution of European soils and groundwater. *National Institute of Public Health and Environmental Protection (RIVM) Report 4615001002*, Bilthoven, The Netherlands.

Turc L, 1954. The water balance of soils. Relation between precipitation, evaporation and flow. *Annales Agronomiques* 5: 491–569.

Van Deursen W P A, 1995. Geographical information systems and dynamic models; development and application of a prototype spatial modelling language. Ph.D. Thesis, Utrecht University. *NGS Publication* 190, 206 pp (Electronically availabel through www.carthago.nl.

Wendland F, 1992. *Die Nitratbelastung in den Grundwasserlandschaften der, alten' Bundesländer (BRD). Berichte aus der Okologischen Forschung*, Band 8, Forschungszentrum Jülich: Jülich; 150 pp.

Appendix 1

Input file processing and output files

Input file processing – Forsmark.

Data type (underlined) and file(s)/ datasets used as a basis for processing	Processed file used as input in the modelling	Comment
Sea, lake and stream locations		
vatten.shp	seamodified.dat	Maps of sea and lake extents were extracted from “vatten.shp” and converted to ArcGIS raster files
hydrografi.shp	strms.dat	The stream locations in “hydrografi.shp” were converted to ArcGIS raster file
Digital elevation model		
dem4_land.dat strms.dat (stream location) seamodified.dat (lake location)	dem4_1filld.txt*	The original DEM was lowered 3 m and 1 m at the location of the streams and lakes, respectively. The pits were filled using ArcGIS Hydrology modeling tool extension.
Precipitation		
TR-02-02	rain.txt*	Spline interpolation using the four precipitation measurement points Lövsta, Risinge, Untra, Örskär, see R-04-54
Precipitation (seasonal)		
TR-02-02	rainsummer.txt*	Spline interpolation of cumulative average precipitation during summer months, June – September, using the four points, Lövsta, Risinge, Untra, Örskär, see R-04-54
TR-02-02	rainwinter.txt*	Spline interpolation of cumulative average precipitation during winter months, October – May, using the four points, Lövsta, Risinge, Untra, Örskär, see R-04-54
Temperature		
TR-02-02	tempannu.txt* (annual mean) tempjanu.txt (January mean)	Spline interpolation using the four temperature measurement points Films Kyrkby, Risinge, Untra, Örskär, see R-04-54
Soil		
j12ino.shp j13iso.shp jordarter.shp	texture.txt*	From j12ino.shp and j13iso.shp, the original soil categories were reduced to five soil texture classes, one peat class and one water class. In the regions where more detailed information were available from jordarter.shp, the same classes were reduced from jordarter.shp.
Vegetation (land cover)		
markdata_12ino_13iso.shp Sankmark_och_berg_i_dagen.shp	landcover.txt*	The original vegetation categories were reduced to four landcover classes and one water class. Then rock and wetland categories extracted from “Sankmark_och_berg_i_dagen. shp” were used as built-up/rock and wetland classes, respectively.

* Also submitted to SKB in electronic format.

Input file processing – Simpevarp.

Data type (underlined) and file(s)/ datasets used as a basis for processing	Processed file used as input in the modelling	Comment
Sea, lake and stream locations		
markytor.shp	seas.shp	Maps of sea and lake extents were
	lakes.dat	extracted from “markytor.shp”
hydrografi.shp	strms.dat	The stream locations in “hydrografi.shp” was converted to the raster file “strms.dat”.
Digital elevation model		
simpevarp_dem.dat strms.dat (stream location) seas.shp lakes.dat (lake location)	oskdem_1fild.txt*	After separation of land using seas.shp, the original DEM was lowered 3 m and 1 m at the location of the streams and lakes, respectively. The pits were filled using ArcGIS Hydrology modeling tool extension.
Precipitation		
data in TR-02-03 and spatial coordinates from Simpevarp_stations-meteorologi_punkt.shp	rain.txt*	Linear interpolation and extrapolation of data from the three measurement points Målilla, Oskarshamn and Ölands N Udde (extrapolation used in the northernmost region due to lack of nearby precipitation data**).
Precipitation (seasonal)		
TR-02-03	rainsummer.txt*	Linear interpolation and extrapolation of cumulative average precipitation during summer months, June – September, from three points, Målilla, Oskarshamn and Ölands N Udde (extrapolation used in the northernmost region due to lack of nearby precipitation data**).
TR-02-03	rainwinter.txt*	Linear interpolation and extrapolation of cumulative average precipitation during winter months, October – May, from three points, Målilla, Oskarshamn and Ölands N Udde (extrapolation used in the northernmost region due to lack of nearby precipitation data**).
Temperature		
TR-02-03 complemented with Västervik data from the SMHI journal *Väder och vatten*	tempannu.txt* (annual mean) tempjanu.txt (January mean)	Spline interpolation using the four temperature measurement points Målilla, Oskarshamn and Ölands N Udde and Västervik.
Soil		
SDEADM_SGU_SM_GEO_2502.shp	texture.txt*	The original soil categories were reduced to five soil texture classes, one peat class and one water class. In two (limited) regions, the model area extended beyond the soil map area. Then, the most predominant soil class of the adjacent region was assigned.
Vegetation (land cover)		
SDEADM_SWP_OSK_BIO_1251.shp	landcover.txt*	The original vegetation categories were reduced to four landcover classes and one water class.

* Also submitted to SKB in electronic format.

** See comment in Section 6.2.

Output files – Forsmark and Simpevarp.

Data type (underlined) and file(s)/ datasets used as a basis for processing	Processed file used as input in the modelling	Comment
Actual evapotranspiration, E_a (annual mean)		
rain.txt, tempannu.txt	eact1.dat	using E_a-method (i), see R-04-54
rain.txt, texture.txt, landcover.txt	eact2.dat	using E_a-method (ii), see R-04-54
rain.txt, texture.txt, landcover.txt	eact2cal.txt*	using E_a-method (ii) calibrated in this study considering site-specific conditions, see Sections 3.1, 5.5 and 7.5.
Actual evapotranspiration, E_a (seasonal mean)		
eact1.dat	eacts.txt*	cumulative evapotranspiration during 4 summer months, June – September, which amounts to 57.5% of annual Ea.
eact1.dat	eactw.txt*	cumulative evapotranspiration during 8 winter months, October – May, which amounts to 42.5% of annual Ea.
Precipitation surplus, PS (annual mean)		
eact1.dat, rain.txt	ps1.dat	matrix operation: (ps1.dat) = (rain.txt)–(eact1.dat)
eact2.dat, rain.txt	ps2.dat	matrix operation: (ps2.dat) = (rain.txt)–(eact2.dat)
eact2cal.txt, rain.txt	ps2cal.txt*	matrix operation: (ps2cal.dat) = (rain.dat)–(eact2cal.dat)
Precipitation surplus, PS (seasonal mean)		
eacts.txt, rainsummer.txt	ps_summer.txt*	cumulative precipitation surplus during 4 summer months, June–September
eactw.txt, rainwinter.txt	ps_winter.dat*	cumulative precipitation surplus during 8 winter months, October–May
Discharge, Q		
ps1.dat	q1.dat	method i based annual discharge
ps2.dat	q2.dat	method ii based annual discharge
ps2cal.txt	q2cal.txt*	calibrated annual discharge
ps_summer.txt	qsummer.txt*	four summer months cumulative discharge
ps_winter.txt	qwinter.txt*	eight winter months cumulative discharge

* Also submitted to SKB in electronic format.